Sources: Magnetohydrodynamic Waves

- Introduction to MHD waves (and beyond)

Dong-Hun Lee
School of Space Research
Kyung Hee University, Korea

Introduction

- Space: *in situ experiment*
- Space is NOT empty and well structured.
- Space has all kinds of dynamics:

Single-ptl + Kinetic + Fluid approach

L ~ 100,000km

dL ~ 100km

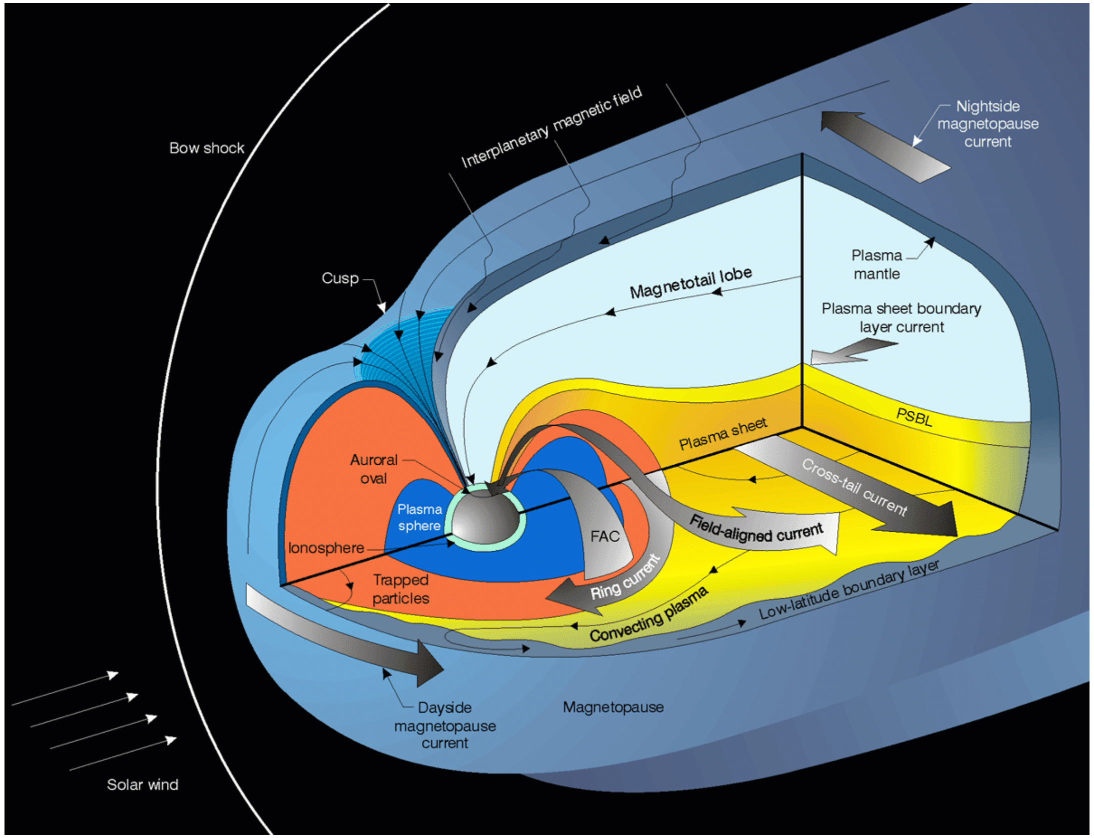

Introduction

(ground)

Sea: $\sim 10^{+22} / cm^3$

Air: $\sim 10^{+19} / cm^3$

- collisions dominant
- diffusive
- neutral ptls
- mech. + gravit.

(space)

$\sim 10^{-2} - 10^{+3} / cm^3$

- collisions negligible
- well-structured
- plasma (ions, electrons)
- mech. + electromag.

cf) For CLIC beams,

$$n_e \sim 10^{12\sim13} / (1nm, 40nm, 150ns * c) \sim 10^{21} / cm^3$$

Background: from single-ptl to fluid

- **Single-ptl** ***(e.g., f=ma)***

$$\vec{X}(t),\ \vec{V}(t) \qquad \vec{F} = m\frac{d\vec{V}}{dt} = q(\vec{E} + \vec{V}\times\vec{B})$$

- **A few or many ptls** ***(kinetic approach, f(x,v,t))***

$$N(\vec{x},\vec{v},\vec{t}) = \sum_j \delta(\vec{x} - \vec{X}_j(t))\ \delta(\vec{v} - \vec{V}_j(t)) \qquad f(\vec{x},\vec{v},t) \equiv < N(\vec{x},\vec{v},t) >$$

- **Multi-fluids** ***(multi-ions + electrons)***

$$n_j(\vec{x}, t),\ \vec{V}_j(\vec{x}, t), P_j(\vec{x}, t), T_j(\vec{x}, t) \qquad j = e, i$$

- **Single-fluid** ***(MHD)*** $n(\vec{x}, t),\ \vec{V}(\vec{x}, t), P(\vec{x}, t), T(\vec{x}, t)$

- **Ideal MHD**

Background: Multi-fluids *(multi-ions + electrons)*

- Multi-fluid equations

$$\frac{\partial n_j}{\partial t} + \nabla \cdot (n_j \mathbf{v_j}) = 0$$

$$m_j n_j \left[\frac{\partial \mathbf{v_j}}{\partial t} + (\mathbf{v_j} \cdot \nabla)\mathbf{v_j} \right] = n_j q_j (\mathbf{E} + \mathbf{v_j} \times \mathbf{B}) - \nabla p_j + \mathbf{R}_j \qquad j = i, e$$

$$p_j = C_j n_j^{\gamma_j}$$

- Ideal MHD equations

$$\frac{\partial n}{\partial t} + \nabla \cdot (n\mathbf{v}) = 0$$

$$mn \left[\frac{\partial \mathbf{v}}{\partial t} + (\mathbf{v} \cdot \nabla)\mathbf{v} \right] = \mathbf{j} \times \mathbf{B} - \nabla p$$

$$p = Cn^{\gamma}$$

$$\mathbf{E} + \mathbf{v} \times \mathbf{B} = 0$$

Approximations

- From *N(x,v,t)* to *f(x,v,t)* :

Neglect the single-particle nature

$$r >> \lambda_D = \sqrt{\frac{\epsilon_o k_B T}{n e^2}} \quad = \text{ the Debye length}$$

$$\Lambda = n{\lambda_D}^3 \;\; >> \;\; 1 \quad : \text{ the plasma parameter}$$

cf) For CLIC beams: $r \gg \lambda_D \;, \;\text{but}\;\; \Lambda \ll 1$

-From *f(x,v,t) {plasma kinetic eq.}* to *f(x,v,t) {Vlasov eq.}*:

Neglect *collisions (resistivity)*
weak turbulence
quasi-linear theory
……

Approximations

- From *f(x,v,t)* to *MF(x,t)* :

Neglect the velocity distribution

ex) wave-particle interaction
microscopic instabilities
Landau damping
non-thermal equilibrium

- From *MF(x,t)* to *SF(x,t)* :

Neglect the electron inertia and the ion species

ex) rapid EM & ES variations

$$\omega < \omega_{ci} = \frac{eB}{m_i}$$ **Ion gyro-frequency**

$$r > r_{ci} = \frac{v_\perp}{\omega_{ci}}$$ **Ion gyro-radius**

Application – Waves in space

<MHD waves>

- ***very low freq:*** ***MHD waves*** $\omega \ll \Omega_i$

<multi-fluid waves>

- ***low freq:*** ***Ion waves*** $\omega \sim \Omega_i$
- ***intermed. freq:*** ***Ion-electron waves*** $\Omega_i < \omega < \Omega_e$
- ***high freq:*** ***Electron waves*** $\omega \sim \Omega_e$

<kinetic waves>

- ***e.g. higher harmonics, Bernstein waves, …***

<single-ptl resonances>

- ***e.g. bounce resonance, bounce-drift resonance, …***

Application – Waves in space

Maxwell eqs
+ Ohm's law

$$\begin{aligned}\vec{\nabla}\times(\vec{\nabla}\times\vec{E}) &= -\frac{1}{c^2}\frac{\partial^2\vec{E}}{\partial t^2}-\mu_o\frac{\partial\vec{J}}{\partial t}\\ &= \frac{\omega^2}{c^2}\left(\mathbf{I}+\frac{i\sigma}{\omega\epsilon_o}\right)\cdot\vec{E}\\ &= k^2\epsilon\cdot\vec{E}\end{aligned}$$

For instance, $\vec{B} = B\ \hat{z}\,,$

$$\epsilon = \begin{pmatrix} S & -iD & 0 \\ iD & S & 0 \\ 0 & 0 & P \end{pmatrix}$$

$$\begin{aligned} S &= 1-\sum_j\frac{\omega_{pj}^2}{\omega^2-\omega_{cj}^2}\\ D &= \sum_j\frac{|q_j|/q_j\ \omega_{cj}\omega_{pj}^2}{\omega(\omega^2-\omega_{cj}^2)}\\ P &= 1-\sum_j\frac{\omega_{pj}^2}{\omega^2}\end{aligned}$$

$$\omega_{pj}=\sqrt{\frac{n_jq_j^2}{m_j\epsilon_o}}\qquad \omega_{cj}=\frac{|q_j|B}{m_j}$$

Application – Waves

- **CMA diagram**

<multi-fluid waves>

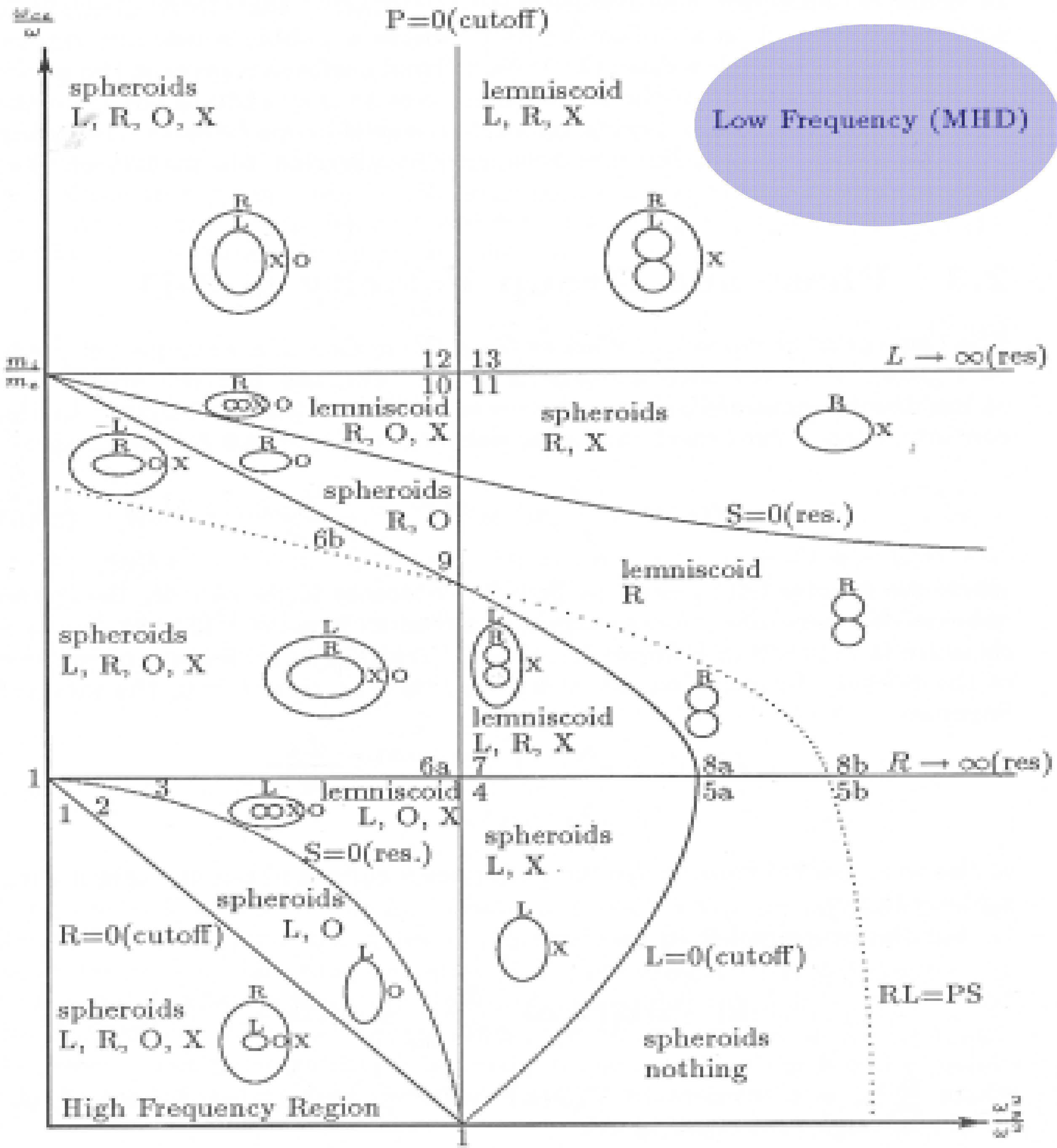

Figure 2.8: CMA diagram with all boundaries and wave normal surfaces.

Application – W

<electron waves>

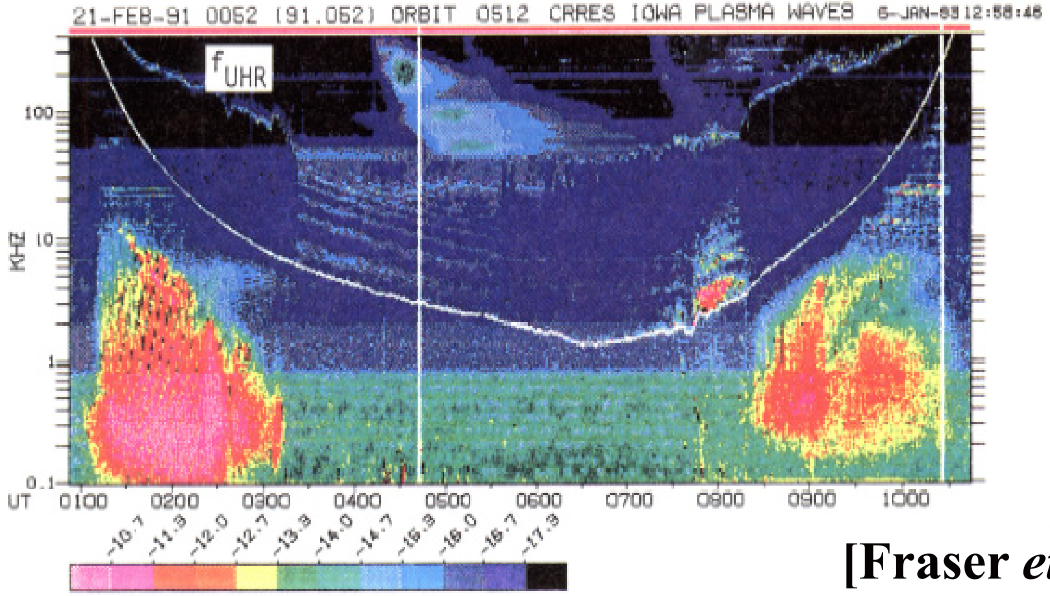

[Fraser *et al.*, 1996]

<multi-ion waves>

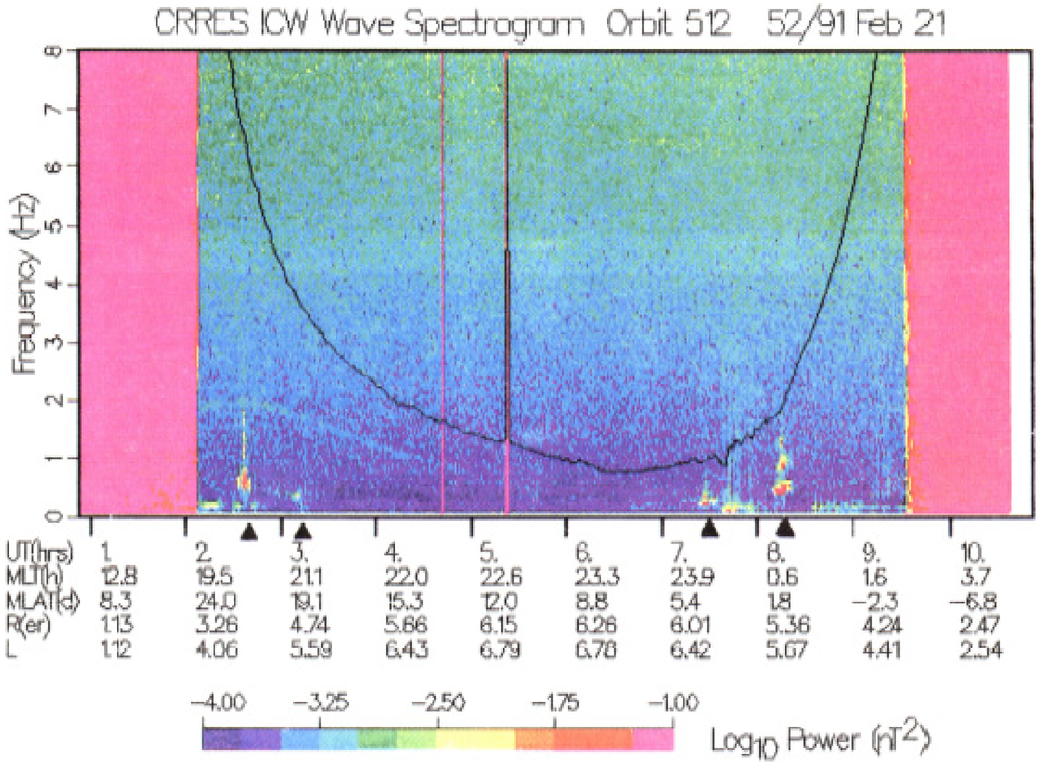

Plate 1. (Upper) CRRES EMIC wave dynamic spectrum for orbit 512 on February 21, 1991. The dark curve is the

Application – Waves in space

- Two wave modes
  - First mode
    - Decreasing frequency with increasing time
  - Second mode
    - Appear after the reception of first wave modes
- Length of the wavetrains grows significantly with z.
- The time delay increases with z.

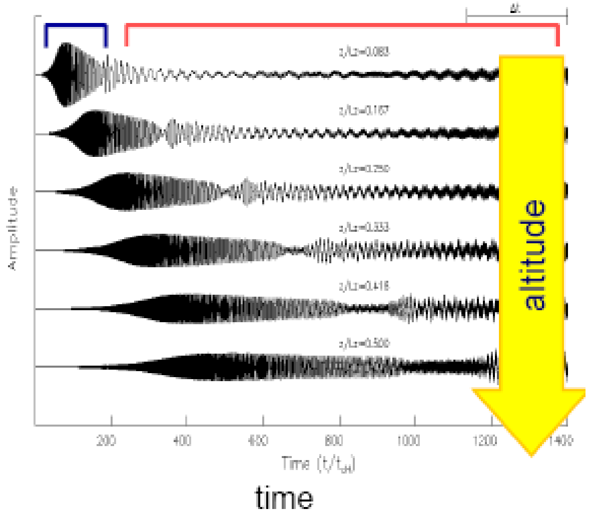

[Kim & Lee, 2005]

<ion-electron waves>

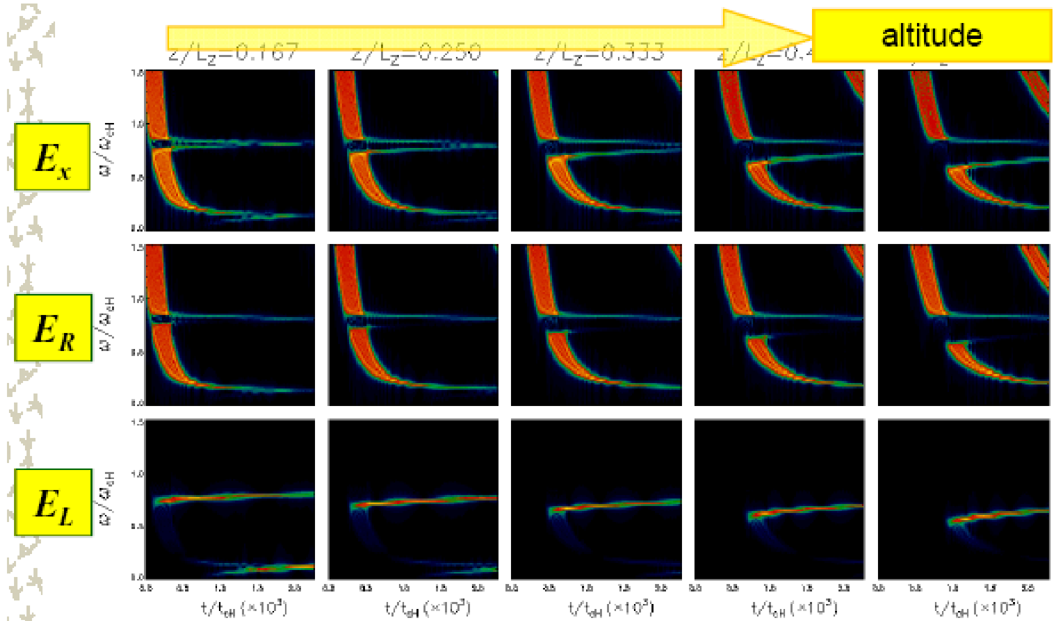

MHD waves

In uniform medium:

$$\omega = \frac{k\,V_A}{\sqrt{1 + \dfrac{i\,k^2}{\mu_o\,\omega\,\sigma}}}$$

- Compressional waves
- Magnetosonic waves
- Isotropic mode
- Three-dimensional

$$\omega = \frac{k_{\parallel}\,V_A}{\sqrt{1 + \dfrac{i\,k^2}{\mu_o\,\omega\,\sigma}}}$$

- Incompressional waves
- Alfven waves
- Anisotropic
- One-dimensional

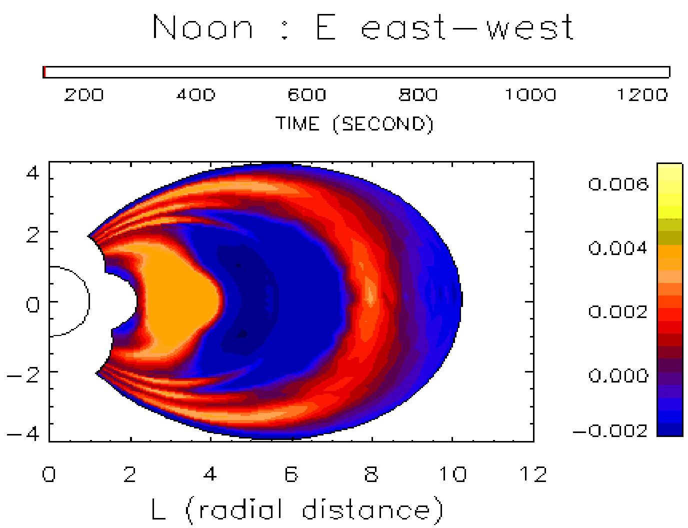

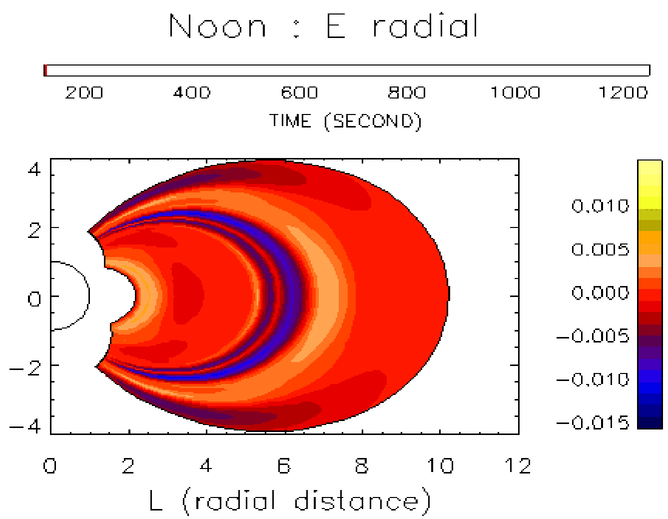

* In a nonuniform plasma,

e.g., MHD waves: $\frac{\omega}{\omega_{cj}} \ll 1$ and $\rho(x), \quad V_A(x) = \frac{B}{\mu_o \rho(x)}$

$$
\begin{aligned}
S &\approx \frac{c^2}{V_A^2} \\
D &\approx 0 \\
P &\rightarrow \infty
\end{aligned}
$$

***Ex* : Alfven waves**
***Ey* : Compressional waves**
***Ez* = 0**

$$\vec{E} \propto e^{i(k_y y + k_z z - \omega t)} \qquad D = \frac{\omega^2}{V_A^2(x)} - k_z^2$$

$$\left(\frac{d}{dx}\frac{D}{D - k_y^2}\frac{dE_y}{dx}\right) + D\,E_y = 0$$

- MHD waves: *Asymptotic solutions*

At resonances,

$$E_x \propto \frac{1}{x - x_0}$$

$$E_y \propto ln|x - x_0|$$

$$\frac{\omega^2}{V_A^2} - k_z^2 = \alpha\,(x - x_0) = C\,(\omega - \omega_0)$$

→ $$E_y(x, t \to \infty) \propto \frac{1}{2\pi}\int_{-\infty}^{\infty} ln|\omega - \omega_0| e^{-i\omega t} d\omega = -\frac{1}{2t} e^{-i\omega_0 t}$$

→ ***Ey*** **is being damped to** ***Ex (even if no dissipations)***

→ **Compressional waves damp, shear Alfven waves grow.**

→ **Resonant absorption of Alfven waves = Field line resonances**

→ ***Mode conversion***

- **Two degrees of freedom become differential in nonuniform plasmas.**
- **In terms of wave (collective) motion, azimuthal or shear motion is stable.**

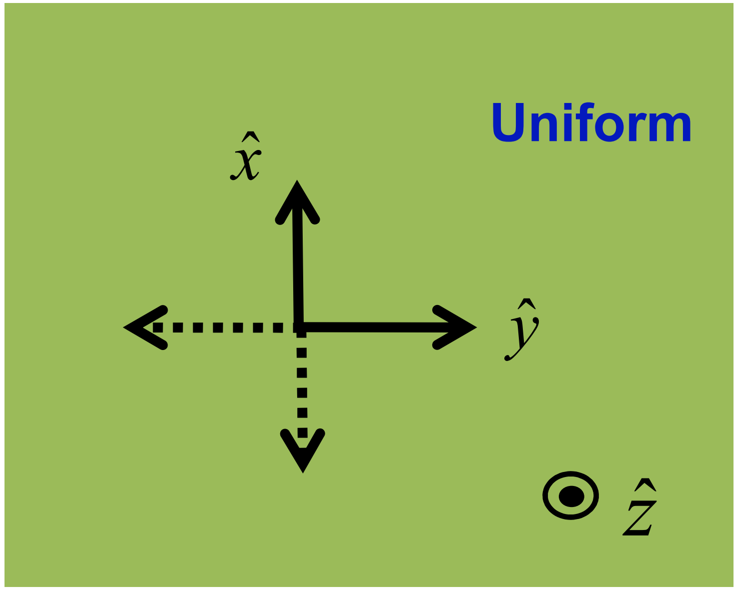

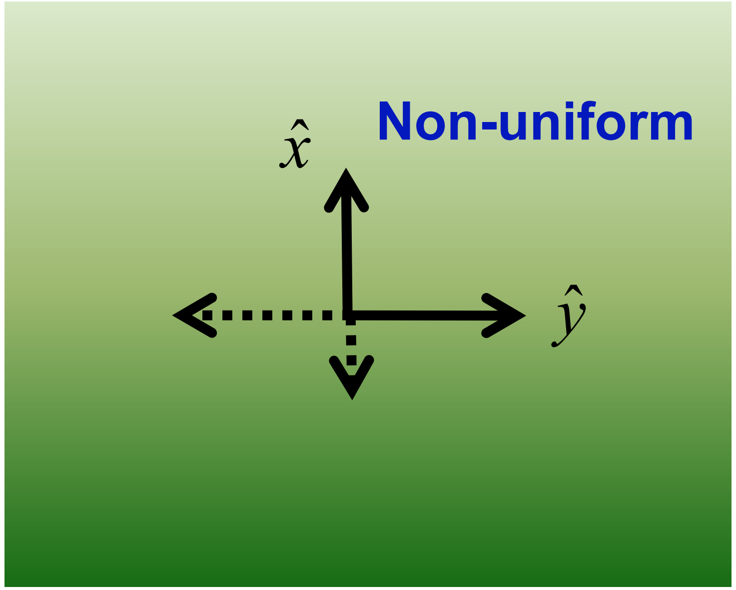

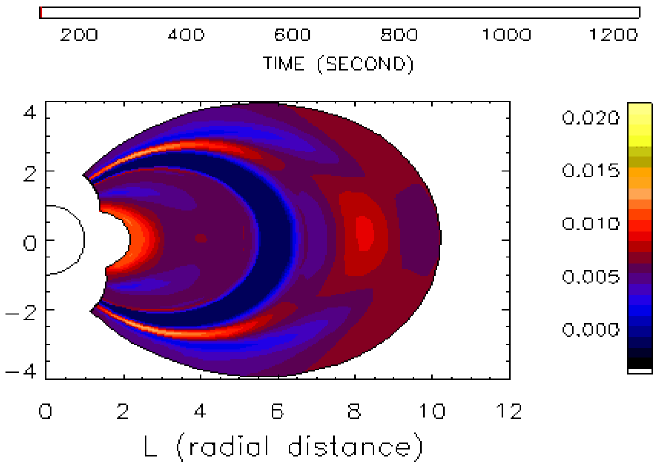

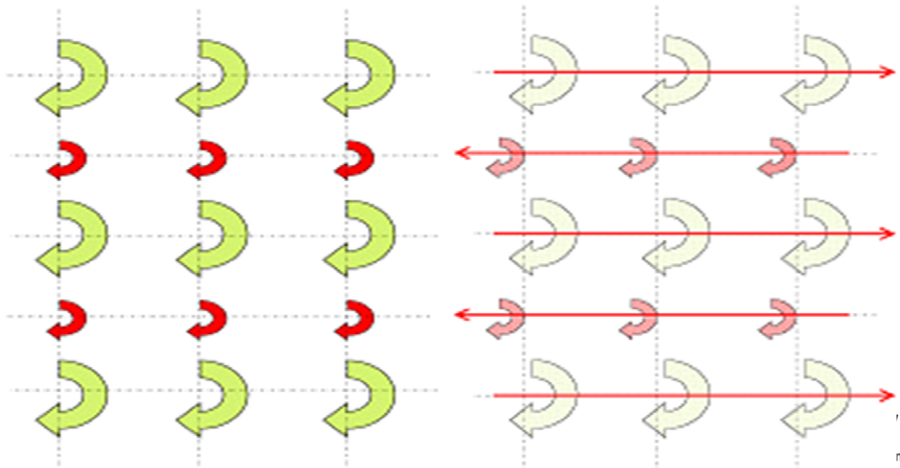

$\vec{E} + \vec{v} \times \vec{B}_o = 0$ **is valid for collective, but relatively low frequency wave motion.**

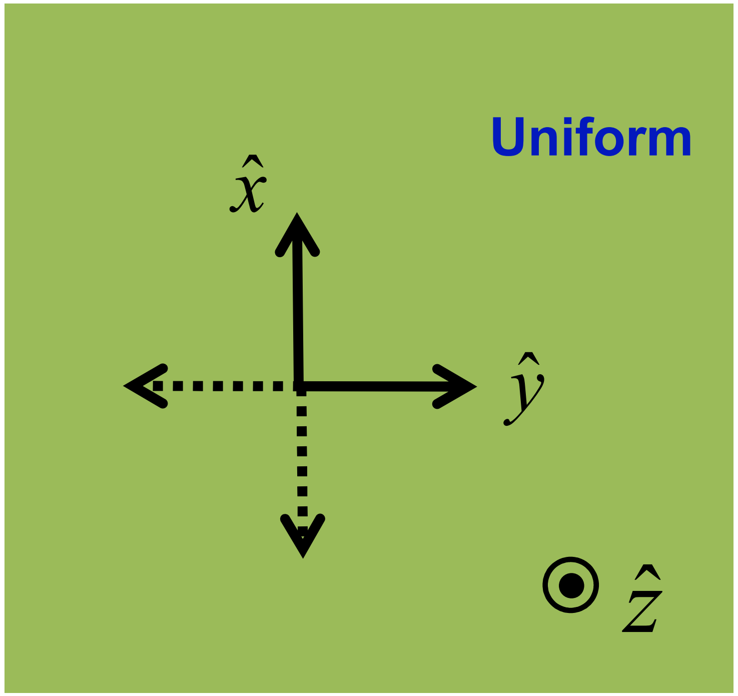

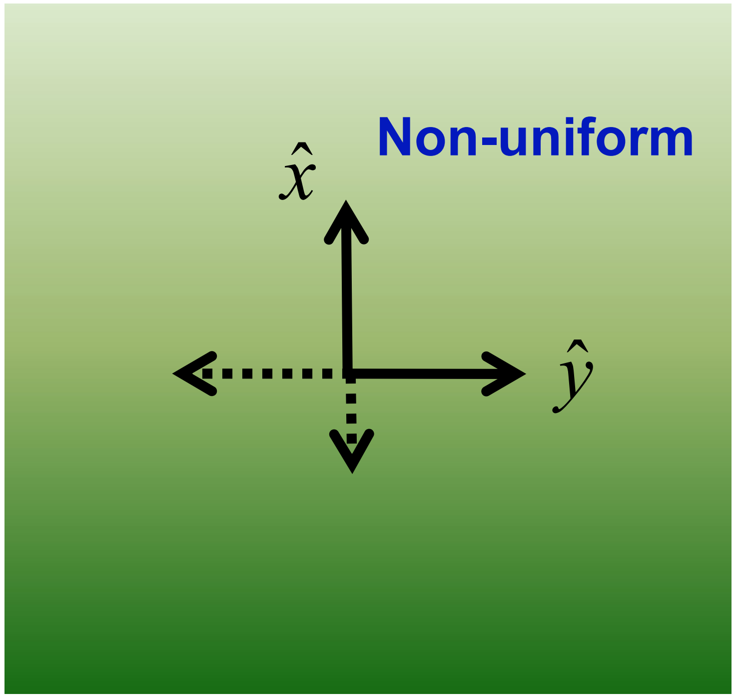

- When inhomo. lies perpendicular to B-field, the azimuthal (shear) motion Vy or radial Ex or azimuthal By are expected to be stable(and dominant?).

* Torodial & Poloidal modes

$$\vec{\nabla}\times\vec{b}=\frac{1}{V_A{}^2(\vec{\mathrm{x}},t)}\frac{\partial \vec{E}}{\partial t}$$

$$\vec{\nabla}\times\vec{E}=-\frac{\partial \vec{b}}{\partial t}$$

$$\varepsilon_\nu = h_\nu E_\nu$$

$$\varepsilon_\varphi = h_\varphi E_\varphi$$

$$h_\mu = \frac{B_E R_E^3}{B_o(\vec{r})} = h_\nu h_\varphi$$

$$h_\nu = \frac{B_E R_E^3}{h_\varphi B_o}$$

$$h_\varphi = r\cos\theta$$

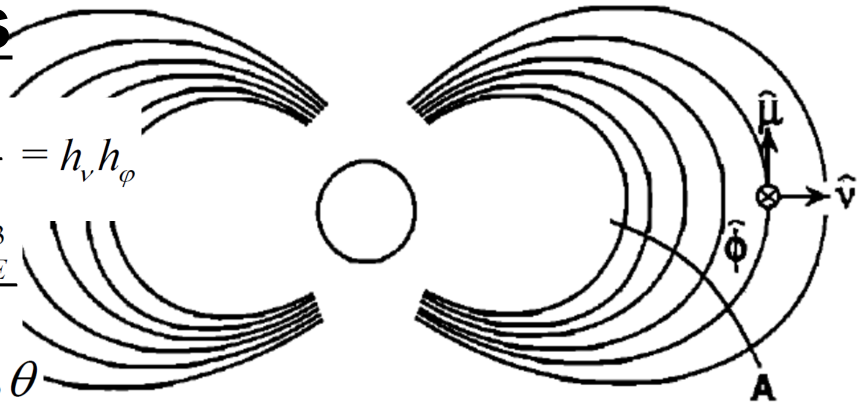

$$\frac{\partial \beta_\mu}{\partial t} = -\left\{\frac{\partial \varepsilon_\varphi}{\partial \nu}-\frac{\partial \varepsilon_\nu}{\partial \varphi}\right\} = -\left\{\frac{\partial \varepsilon_\varphi}{\partial \nu}+im\varepsilon_\nu\right\}$$

In the dipole coordinate $(\mu,\ \nu,\ \varphi)$

$$\left\{\frac{1}{V_A^2}\frac{\partial^2}{\partial t^2}-\frac{1}{h_\varphi^2}\frac{\partial}{\partial \mu}\left(\frac{1}{h_\nu^2}\frac{\partial}{\partial \mu}\right)\right\}\varepsilon_\nu = \frac{1}{h_\varphi^2}\frac{\partial}{\partial \varphi}\left\{\frac{\partial \varepsilon_\varphi}{\partial \nu}-\frac{\partial \varepsilon_\nu}{\partial \varphi}\right\} = \frac{1}{h_\varphi^2}im\left\{\frac{\partial \varepsilon_\varphi}{\partial \nu}+im\varepsilon_\nu\right\}$$

$$\left\{\frac{1}{V_A^2}\frac{\partial^2}{\partial t^2}-\frac{1}{h_\nu^2}\frac{\partial}{\partial \mu}\left(\frac{1}{h_\varphi^2}\frac{\partial}{\partial \mu}\right)\right\}\varepsilon_\varphi = \frac{1}{h_\nu^2}\frac{\partial}{\partial \nu}\left\{\frac{\partial \varepsilon_\varphi}{\partial \nu}-\frac{\partial \varepsilon_\nu}{\partial \varphi}\right\} = \frac{1}{h_\nu^2}\frac{\partial}{\partial \nu}\left\{\frac{\partial \varepsilon_\varphi}{\partial \nu}+im\varepsilon_\nu\right\}$$

$$\left\{\frac{1}{V_A^2}\frac{\partial^2}{\partial t^2}-\frac{1}{h_\varphi^2}\frac{\partial}{\partial \mu}\left(\frac{1}{h_\nu^2}\frac{\partial}{\partial \mu}\right)\right\}\varepsilon_\nu = 0$$

Toroidal: $m = 0$

$$\left\{\frac{1}{V_A^2}\frac{\partial^2}{\partial t^2}-\frac{1}{h_\nu^2}\frac{\partial}{\partial \mu}\left(\frac{1}{h_\varphi^2}\frac{\partial}{\partial \mu}\right)\right\}\varepsilon_\varphi = 0$$

Poloidal: $m \to \infty$

* Torodial & Poloidal modes

[McPherron, 2005]

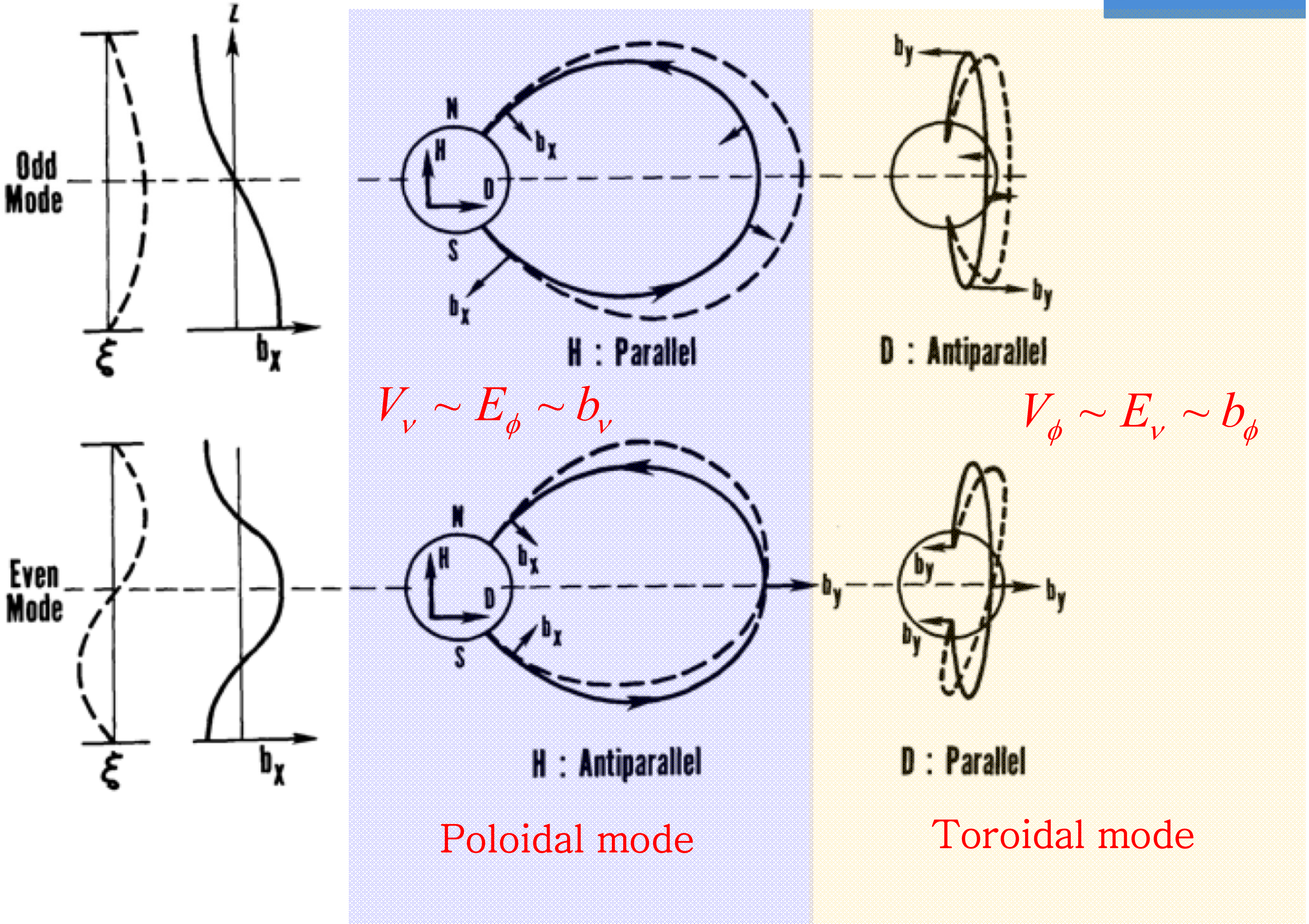

Application – Waves in space

<MHD waves>

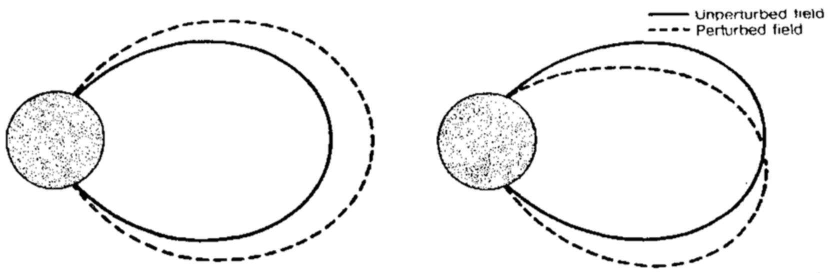

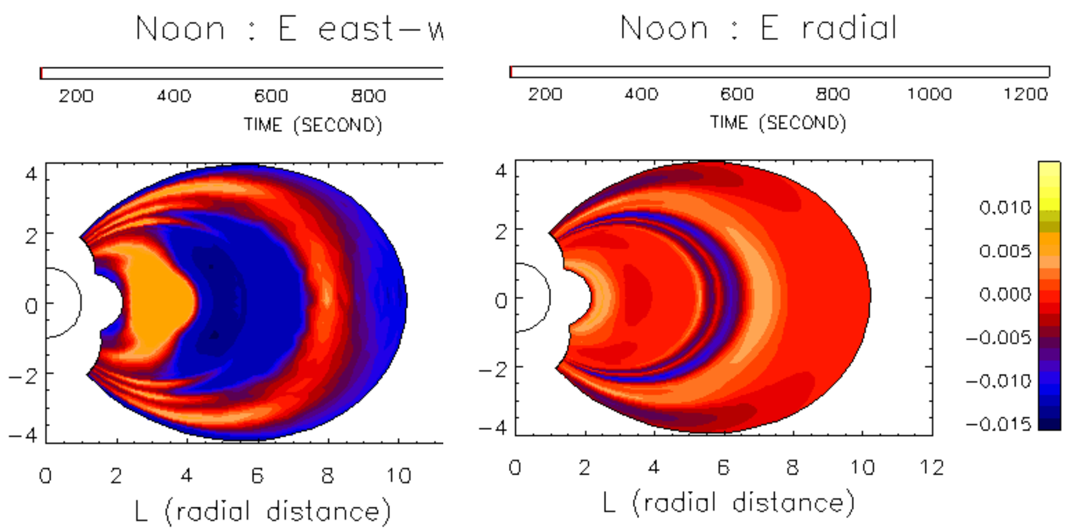

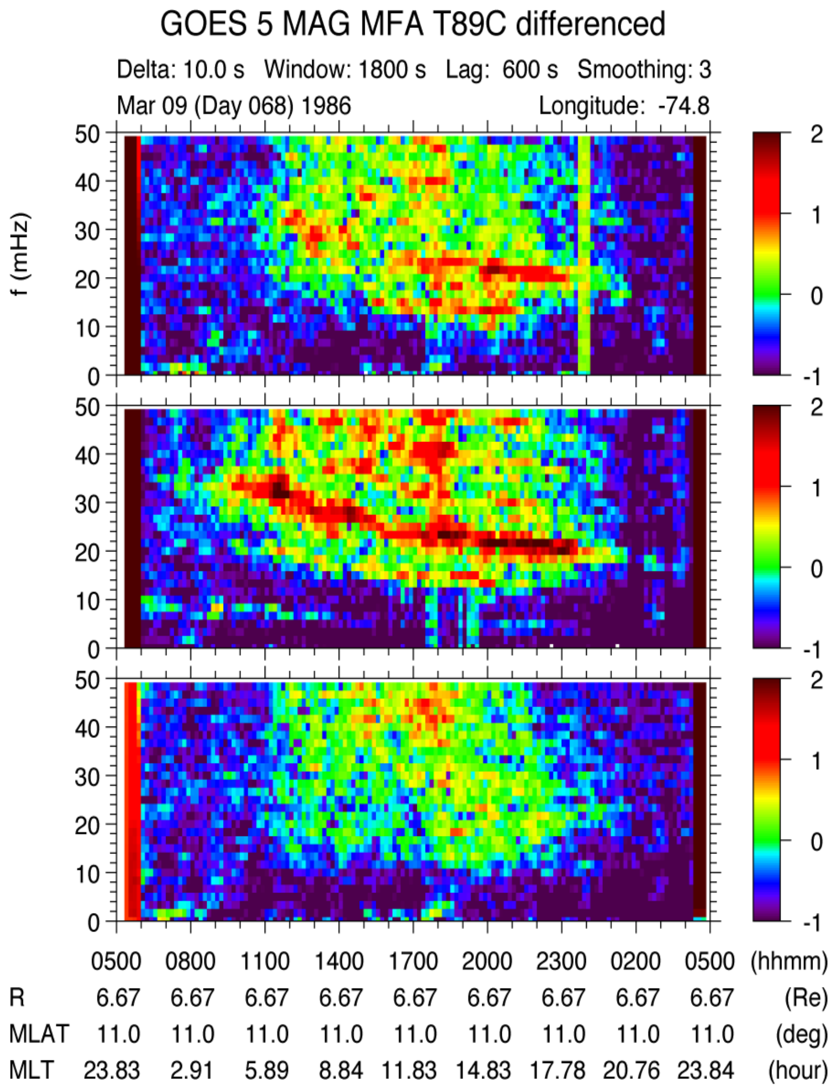

- 3-D dipole MHD waves

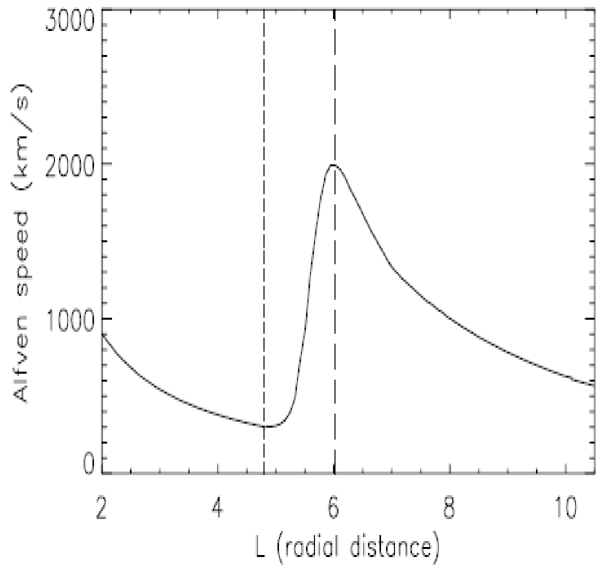

[e.g., Lee *et al.*, 2004]

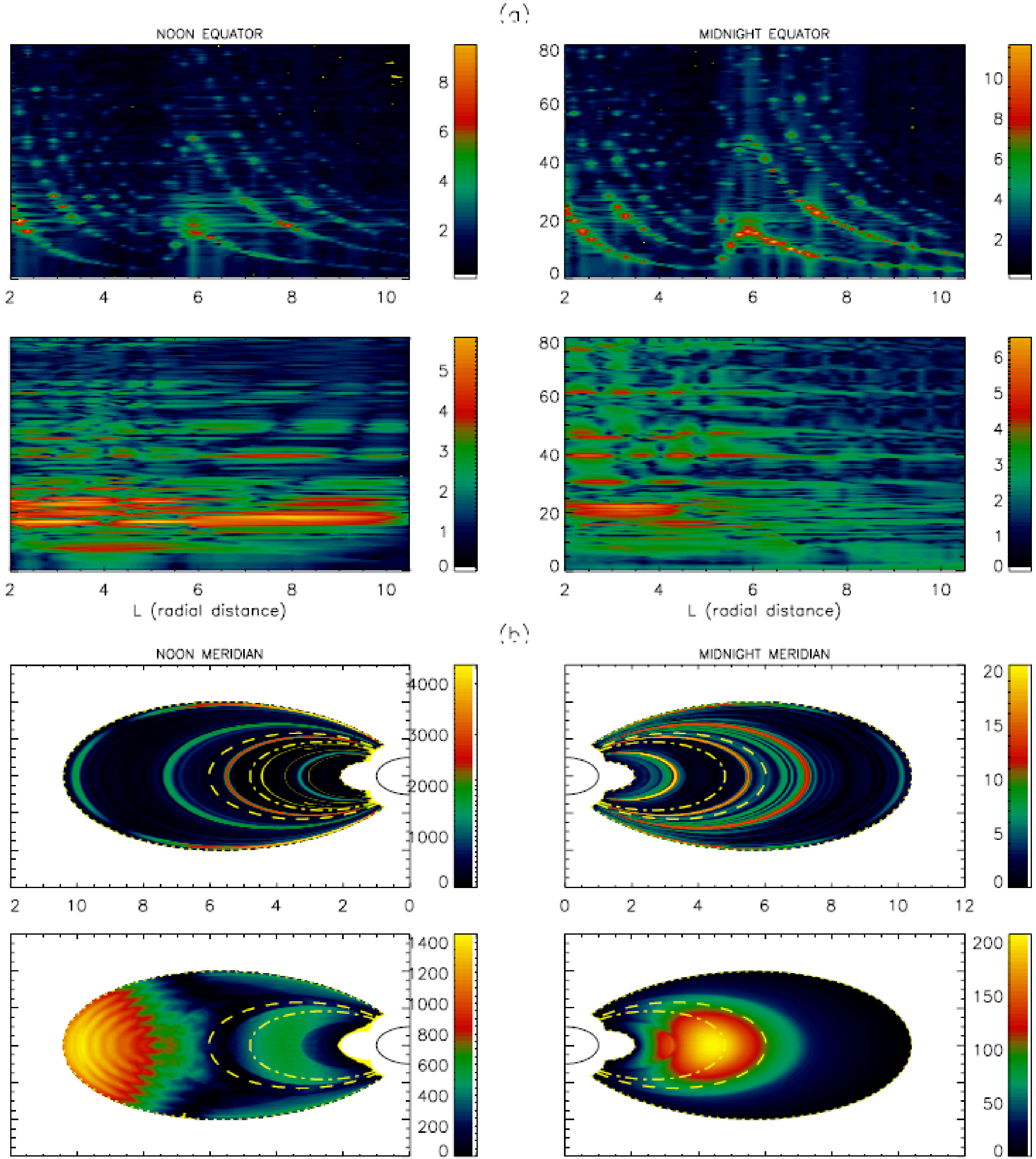

cf) For CLIC,

$\lambda_{lat} \sim 47^o$

$L \sim 2.1\mathrm{Re}$

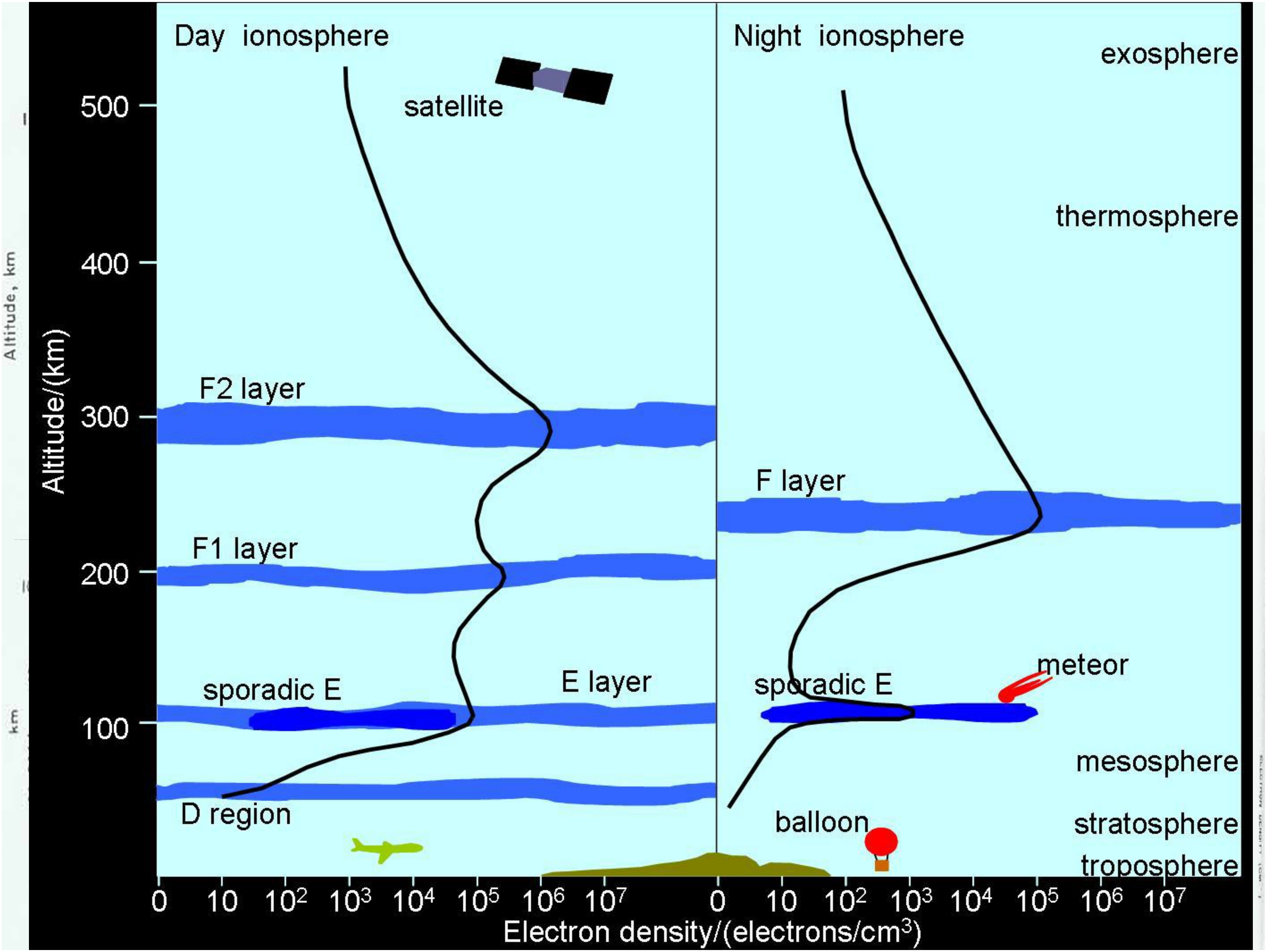

Day ionosphere
Night ionosphere
exosphere
satellite
500
thermosphere
400
Altitude/(km)
F2 layer
300
F layer
F1 layer
200
meteor
sporadic E
E layer
sporadic E
100
mesosphere
D region
balloon
stratosphere
troposphere
0 10 10^2 10^3 10^4 10^5 10^6 10^7
0 10 10^2 10^3 10^4 10^5 10^6 10^7
Electron density/(electrons/cm^3)

Collisions with *neutral* ptls

*** Assume:** $\vec{v}_n = 0$

- Eqs of motion:

$$m_i \frac{\partial \vec{v}_i}{\partial t} = e\left(\vec{E} + \vec{v}_i \times \vec{B}\right) - m_i \nu_{in} \vec{v}_i$$

$$m_e \frac{\partial \vec{v}_e}{\partial t} = -e\left(\vec{E} + \vec{v}_e \times \vec{B}\right) - m_e \nu_{en} \vec{v}_e$$

$$\Longrightarrow \quad \vec{J} = \overleftrightarrow{\sigma} \cdot \vec{E} = \begin{pmatrix} \sigma_P & -\sigma_H & 0 \\ \sigma_H & \sigma_P & 0 \\ 0 & 0 & \sigma_{\parallel} \end{pmatrix} \cdot \begin{pmatrix} E_x \\ E_y \\ E_z \end{pmatrix}$$

$$\Longrightarrow \quad \vec{J} = \sigma_{\parallel} \vec{E}_{\parallel} + \sigma_P \vec{E}_{\perp} - \sigma_H \frac{\vec{E} \times \vec{B}}{B}$$

Collisions with *neutral* ptls

where

$$\sigma_P = \epsilon_o \sum_j \frac{\omega_{pj}{}^2 (\nu_{jn} - i\omega)}{(\nu_{jn} - i\omega)^2 + \omega_{cj}{}^2}$$

$$\sigma_H = -\epsilon_o \sum_j \frac{\epsilon_j\, \omega_{pj}{}^2\, \omega_{cj}}{(\nu_{jn} - i\omega)^2 + \omega_{cj}{}^2}$$

$$\sigma_\parallel = \epsilon_o \sum_j \frac{\omega_{pj}{}^2}{\nu_{jn} - i\omega}$$

If $\omega \ll \nu_{jn}$

$$\sigma_P \cong \epsilon_o \sum_j \frac{\omega_{pj}{}^2\, \nu_{jn}}{\nu_{jn}{}^2 + \omega_{cj}{}^2} = \left(\frac{\nu_{en}}{\nu_{en}{}^2 + \omega_{ce}{}^2} + \frac{m_e}{m_i} \frac{\nu_{in}}{\nu_{in}{}^2 + \omega_{ci}{}^2} \right) \frac{n_e e^2}{m_e}$$

$$\sigma_H \cong -\epsilon_o \sum_j \frac{\epsilon_j\, \omega_{pj}{}^2\, \omega_{cj}}{\nu_{jn}{}^2 + \omega_{cj}{}^2} = \left(\frac{\omega_{ce}}{\nu_{en}{}^2 + \omega_{ce}{}^2} - \frac{m_e}{m_i} \frac{\omega_{ci}}{\nu_{in}{}^2 + \omega_{ci}{}^2} \right) \frac{n_e e^2}{m_e}$$

$$\sigma_\parallel \cong \epsilon_o \sum_j \frac{\omega_{pj}{}^2}{\nu_{jn}} = \left(\frac{1}{\nu_{en}} + \frac{m_e}{m_i} \frac{1}{\nu_{in}} \right) \frac{n_e e^2}{m_e}$$

Collisions with *neutral* ptls

since $$\frac{\sigma_P(j)}{\sigma_H(j)} \approx \frac{\nu_{jn}}{\omega_{cj}}$$

$$\omega_{cj} \ll \nu_{jn} \qquad \sigma_P(j) \gg \sigma_H(j)$$

$$\omega_{cj} \gg \nu_{jn} \qquad \sigma_P(j) \ll \sigma_H(j)$$

$$\frac{\omega_{ce}}{\omega_{ci}} = \frac{m_i}{m_e} = 1836$$

$$\frac{\nu_{en}}{\nu_{in}} = \sqrt{\frac{m_i}{m_n}} = \sqrt{1836} \cong 43$$

There are 3 choices:

$\omega_{ci} \ll \omega_{ce} \lesssim \nu_{in} \ll \nu_{en}$ **: both P currents dominant**

$\omega_{ci} \ll \nu_{in} \ll \nu_{en} \ll \omega_{ce}$ **: P(i) and H(e)**

$\nu_{in} \ll \nu_{en} \ll \omega_{ci} \ll \omega_{ce}$ **: both H currents dominant**

* Ionosphere: *Composition*

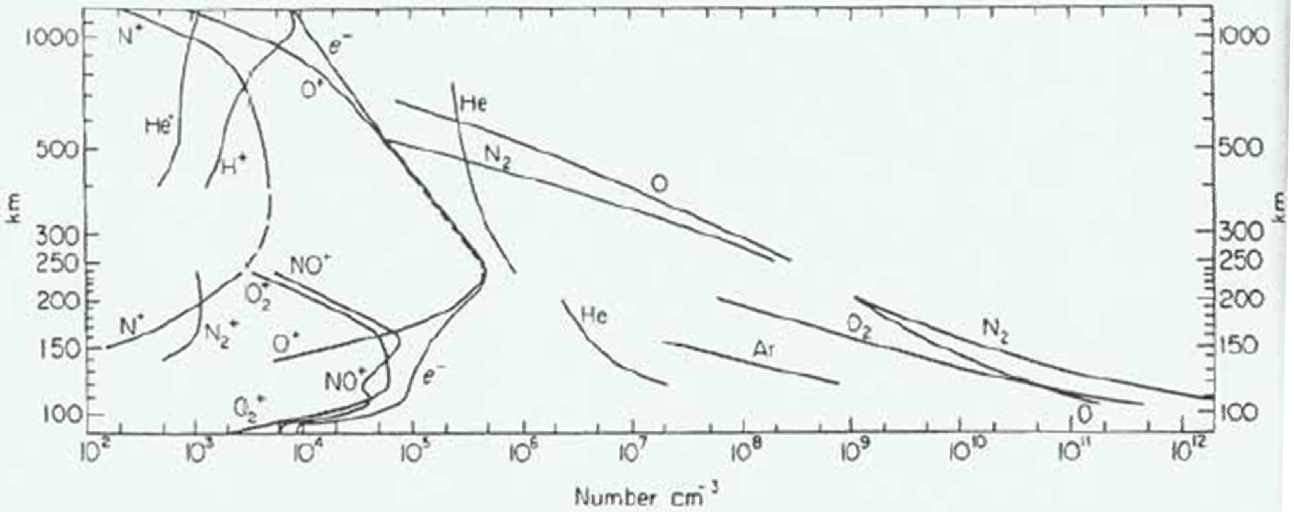

Fig. 1.2. International Quiet Solar Year (IQSY) daytime atmospheric composition, based on mass spectrometer measurements above White Sands, New Mexico (32°N, 106°W). The helium distribution is from a nighttime measurement. Distributions above 250 km are from the Elektron II satellite results of Istomin (1966) and Explorer XVII results of Reber and Nicolet (1965). [C. Y. Johnson, U.S. Naval Research Laboratory, Washington, D.C. Reprinted from Johnson (1969) by permission of the MIT Press, Cambridge, Massachusetts. Copyright 1969 by MIT.]

Collisions with *neutral* ptls

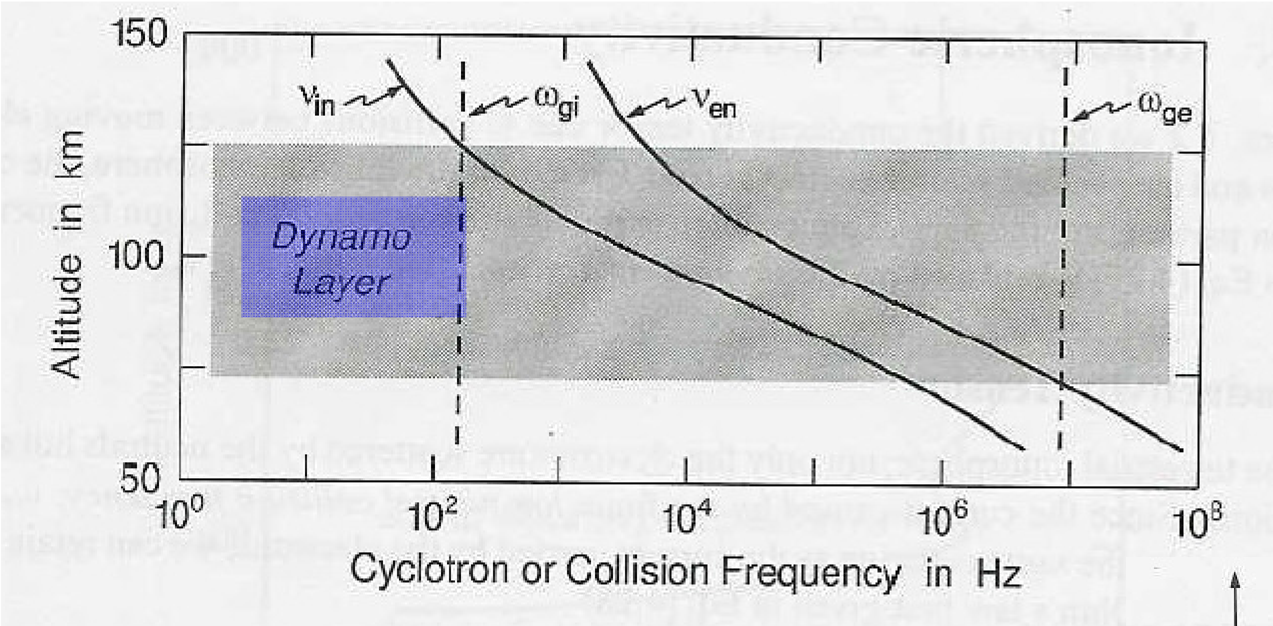

$$\omega_{ci} \ll \nu_{in} \ll \nu_{en} \ll \omega_{ce}$$

(*After* **Baumjohann & Treumann, 1996**)

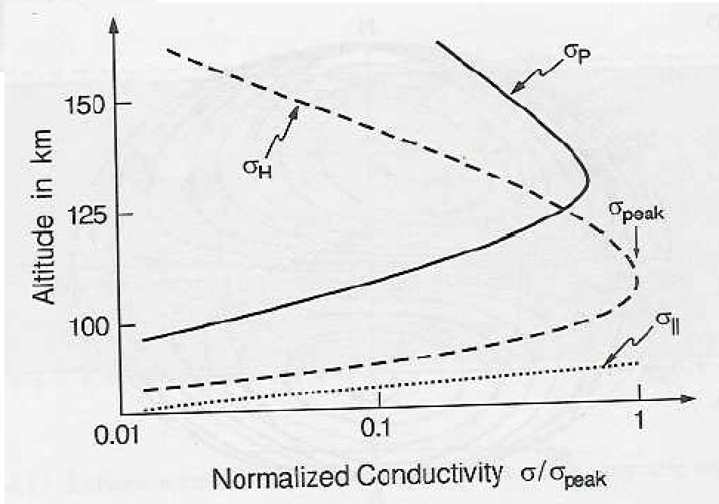

Fig. 4.11. Height profiles of normalized conductivities.

* CME observations at the two near-by stations (< 60km)

- **1996.12.02 09:30 - 10:30(UT) at Icheon, Yongin station**

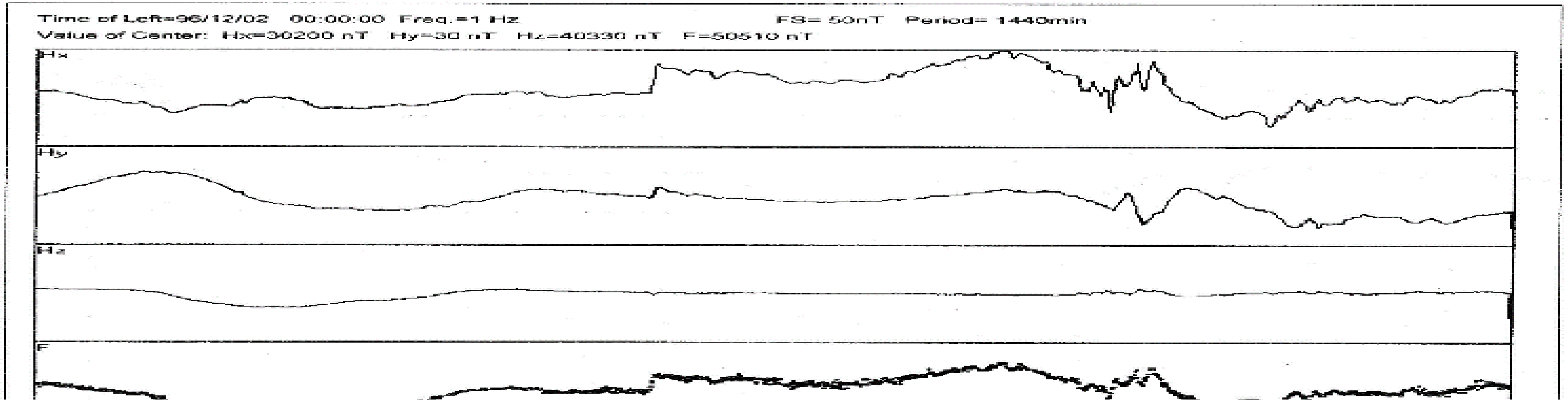

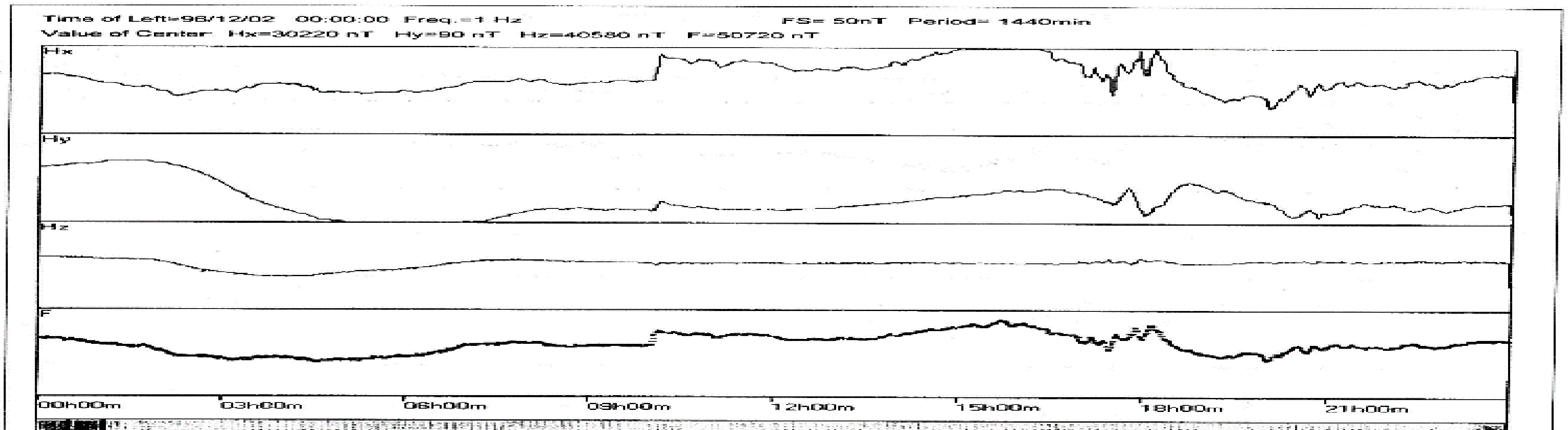

• **daily variations**

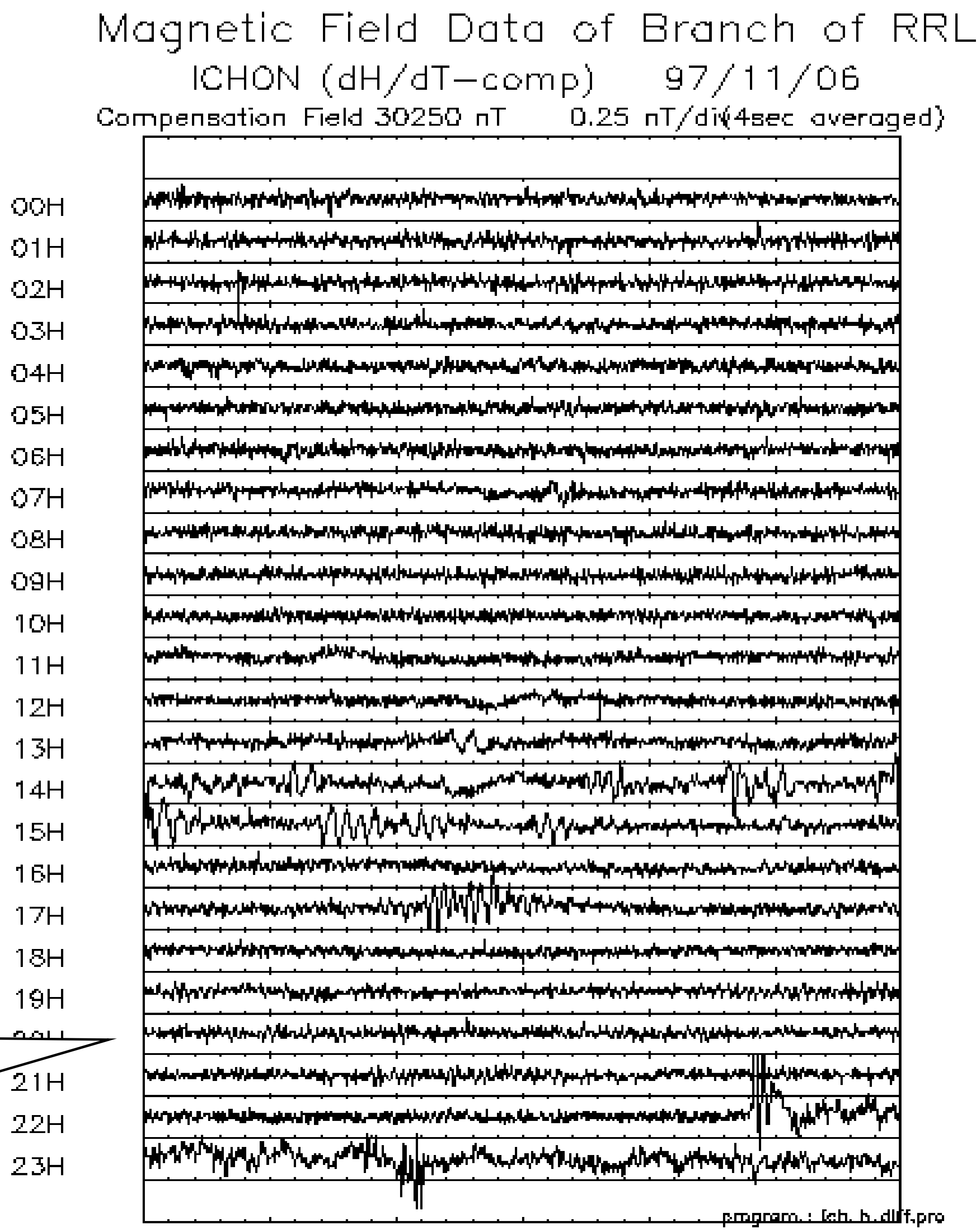

97/11/06
이천 전파연구소
관측자료

Application - Magnetospheric dynamics

❑ 2006년 7월 31일(평온)

[Petrinec, 1994]

❑ 2000년 7월 14일

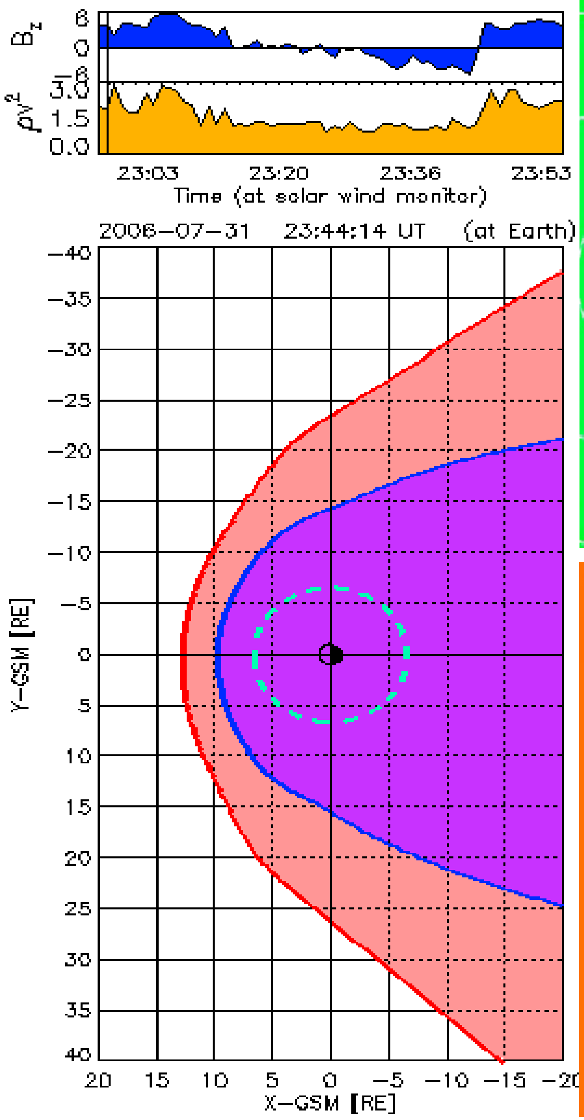

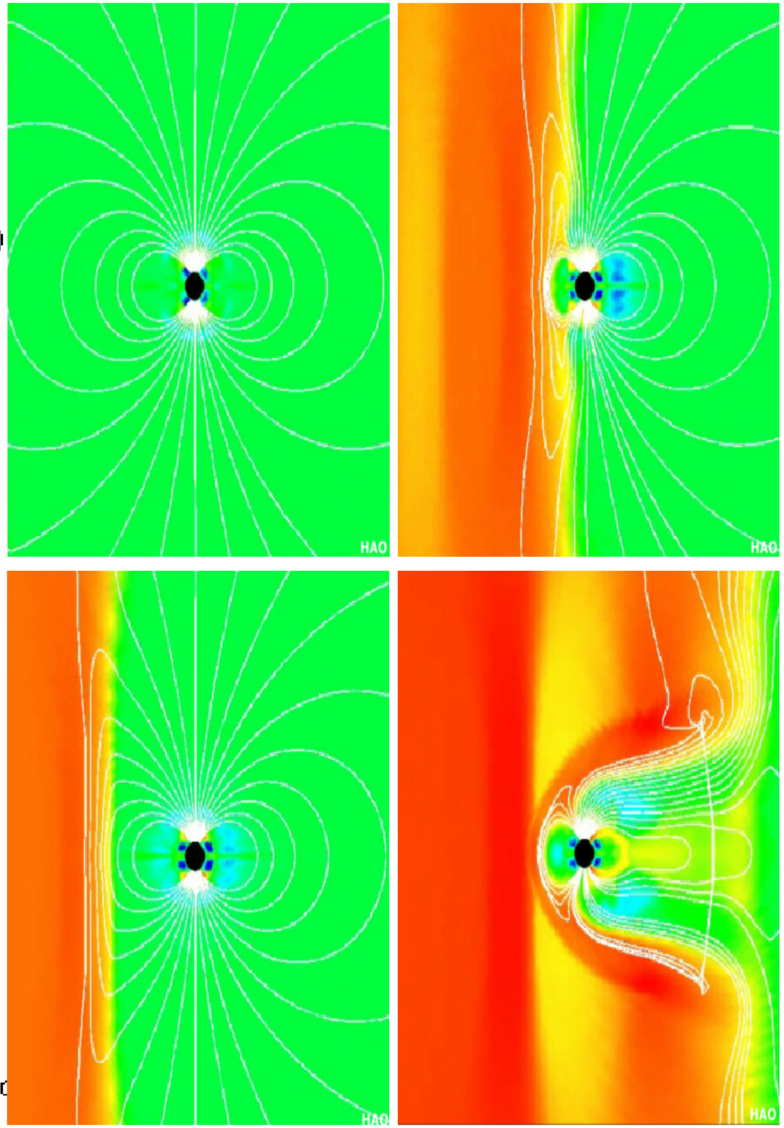

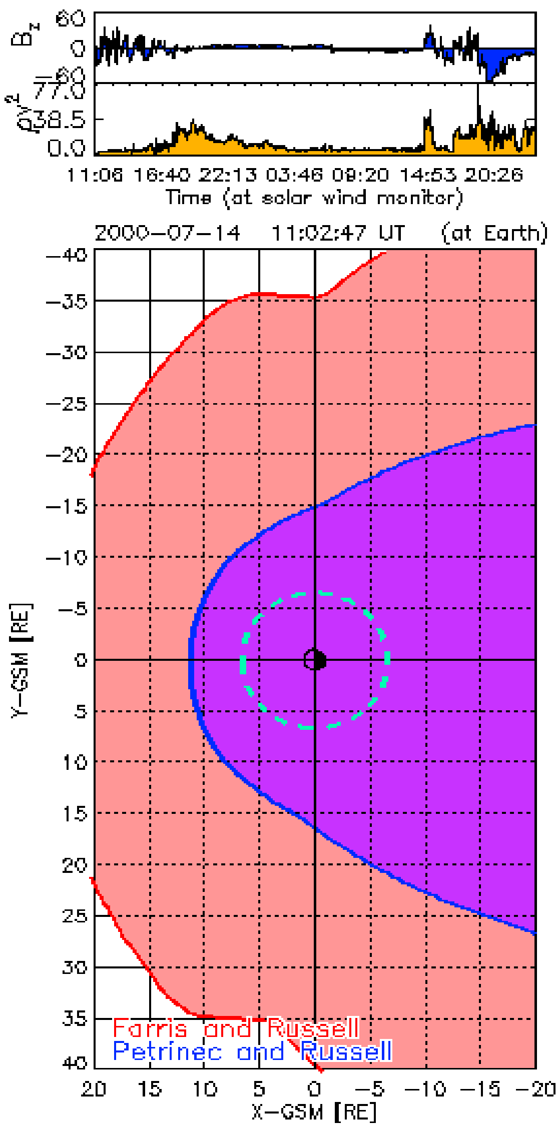

*** MHD Dynamo:** $\vec{E} + \vec{V} \times \vec{B} = 0$ ***(ideal MHD eq.)***

- ***EM energy generates mechanical energy or***
- ***Mechanical energy generates EM energy***

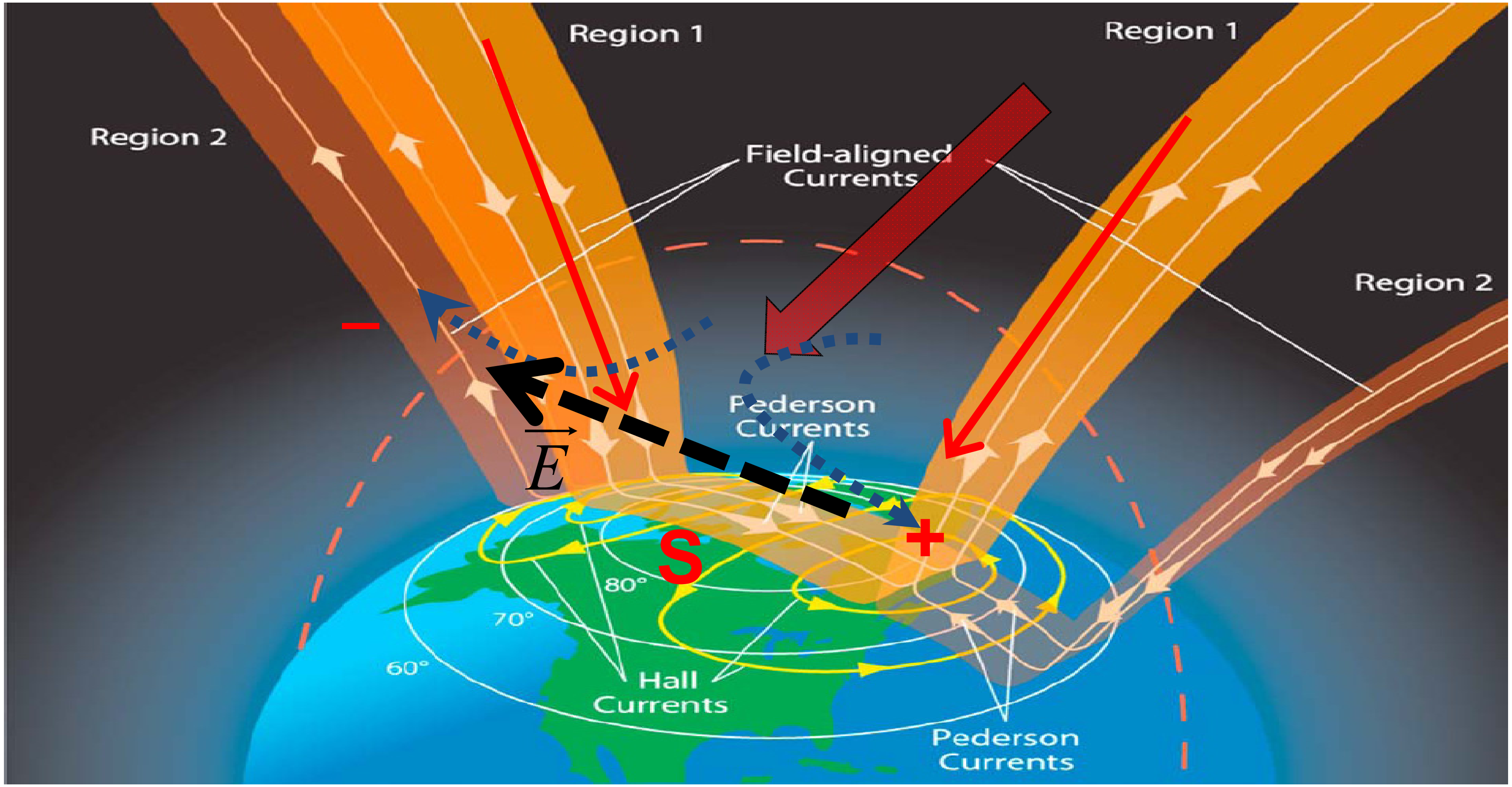

Application
- Magnetospheric dynamics

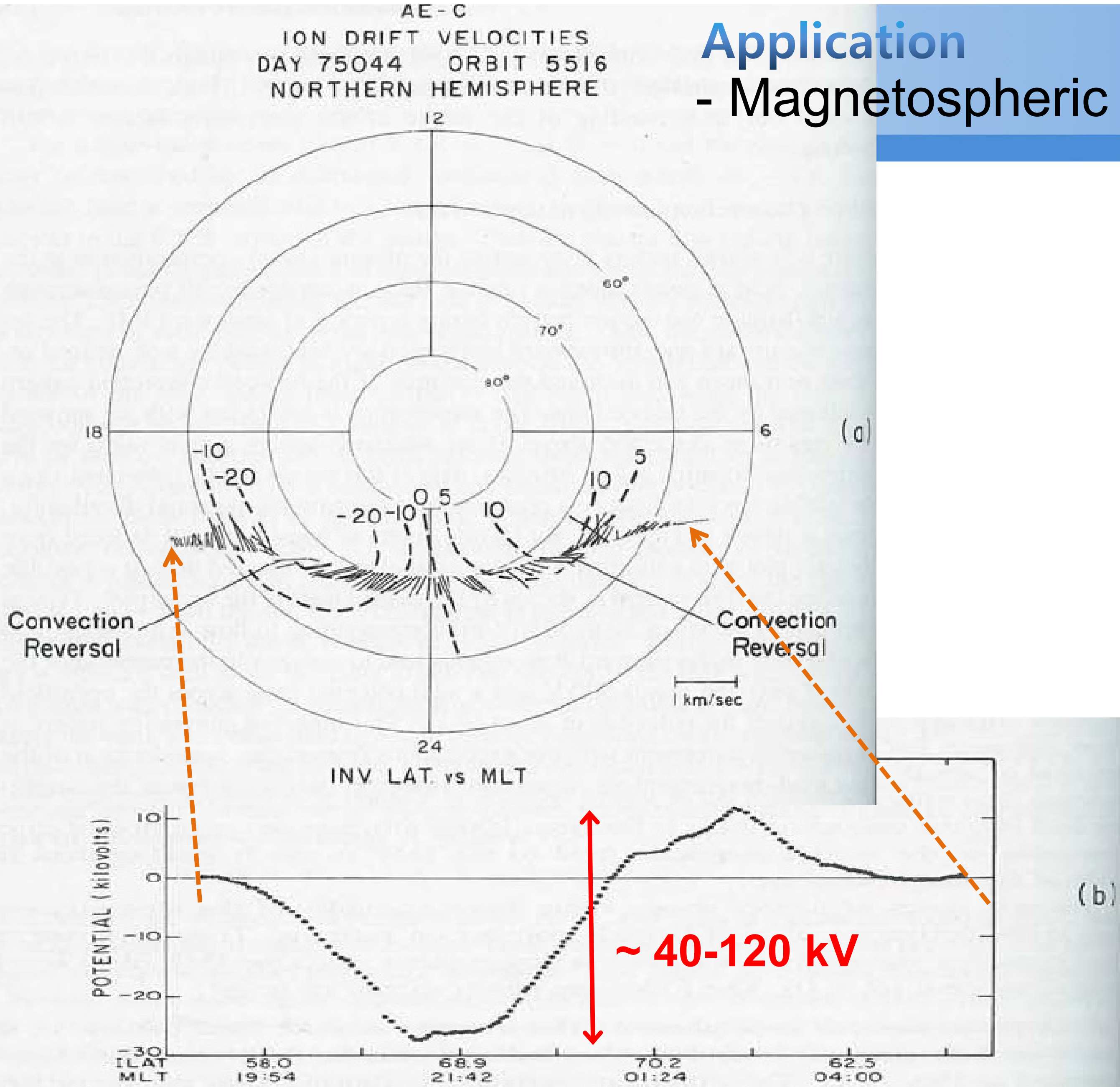

Fig. 6.7. (a) A satellite flight across the high-latitude convection pattern provides drift velocity profiles, which are shown along with the inferred convection pattern. (b) The potential distribution resulting from this convective flow pattern shows maxima and minima at the polar cap boundaries and a total potential difference of about 60 kV across the polar cap. [After Heelis and Hanson (1980). Reproduced with permission of the American Geophysical Union.]

Geomagnetic Induced Currents

1989.3.13

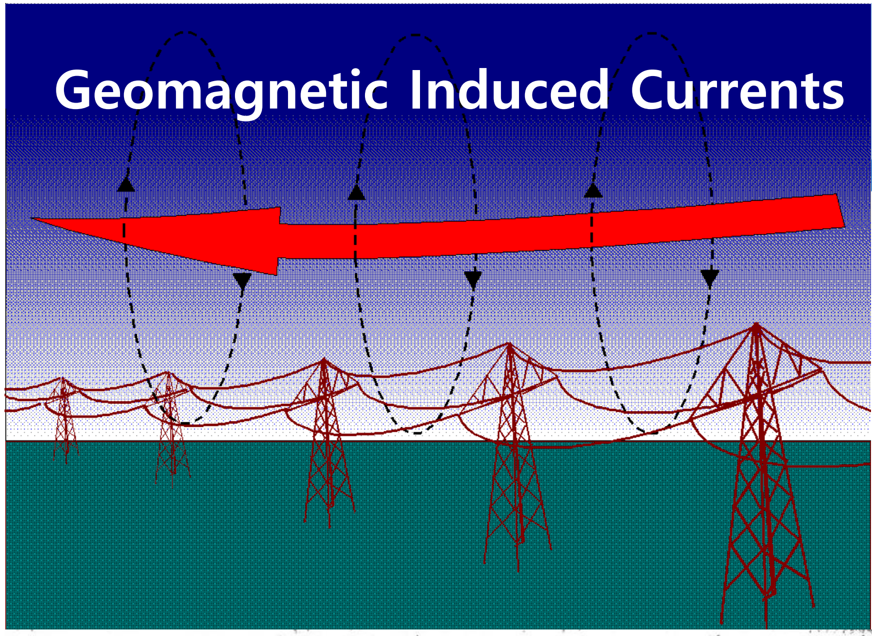

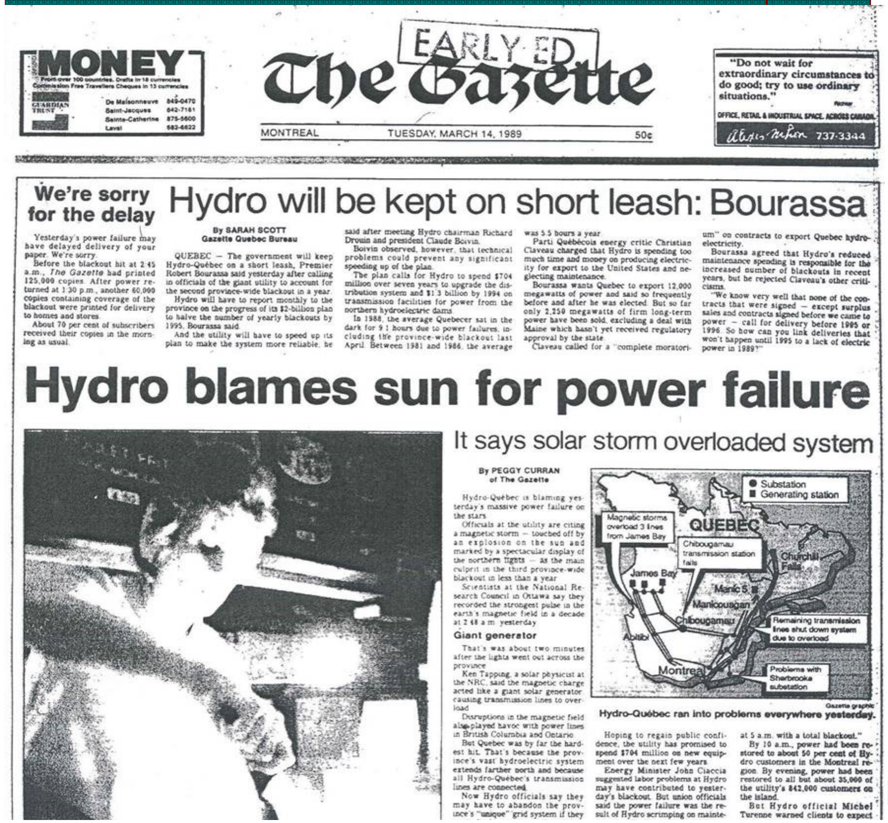

MONEY

The Gazette

EARLY ED.

MONTREAL TUESDAY, MARCH 14, 1989 50¢

"Do not wait for extraordinary circumstances to do good; try to use ordinary situations."

We're sorry for the delay

Hydro will be kept on short leash: Bourassa

Hydro blames sun for power failure

It says solar storm overloaded system

By PEGGY CURRAN of The Gazette

Giant generator

Hydro-Québec ran into problems everywhere yesterday.

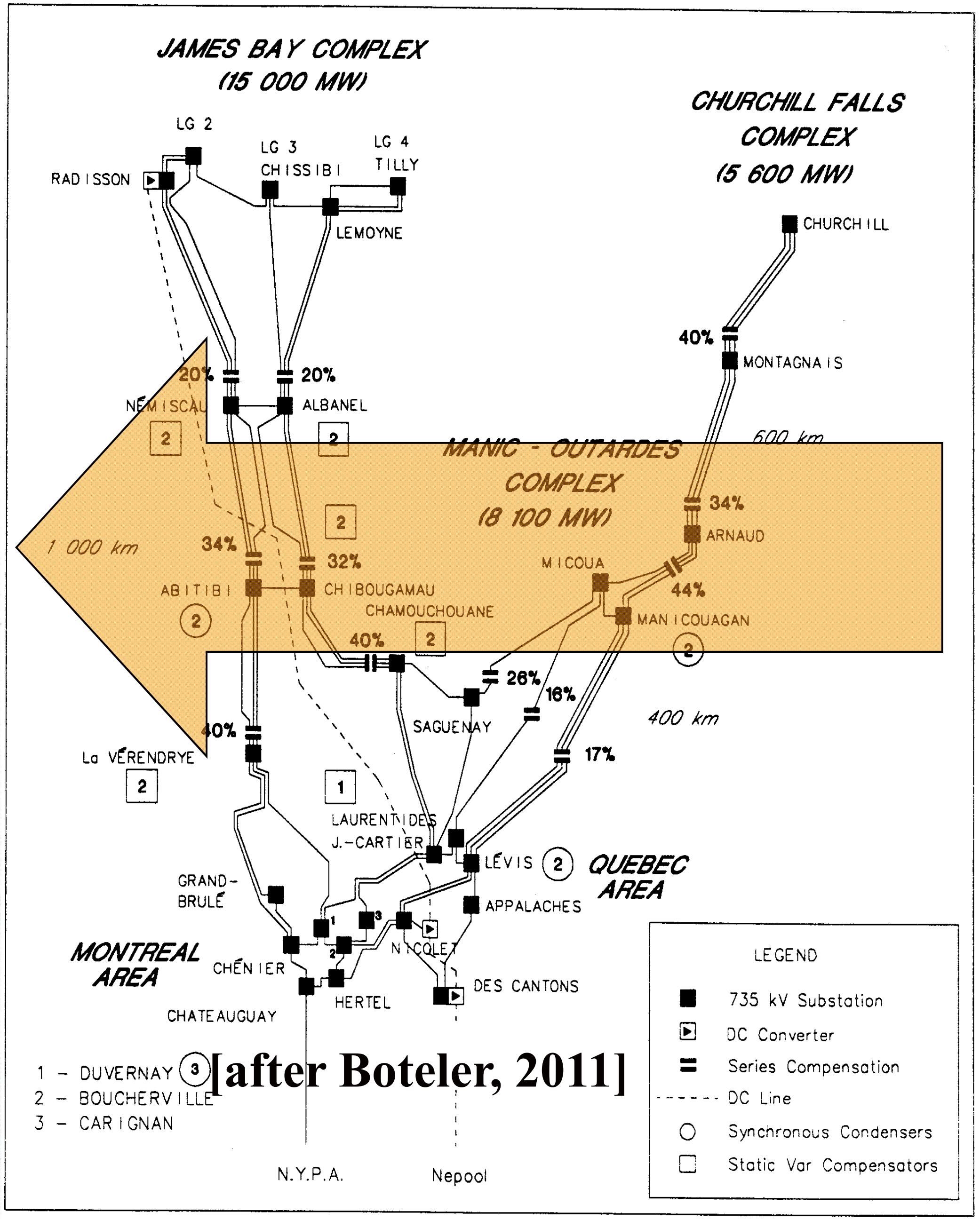

[after Boteler, 2011]

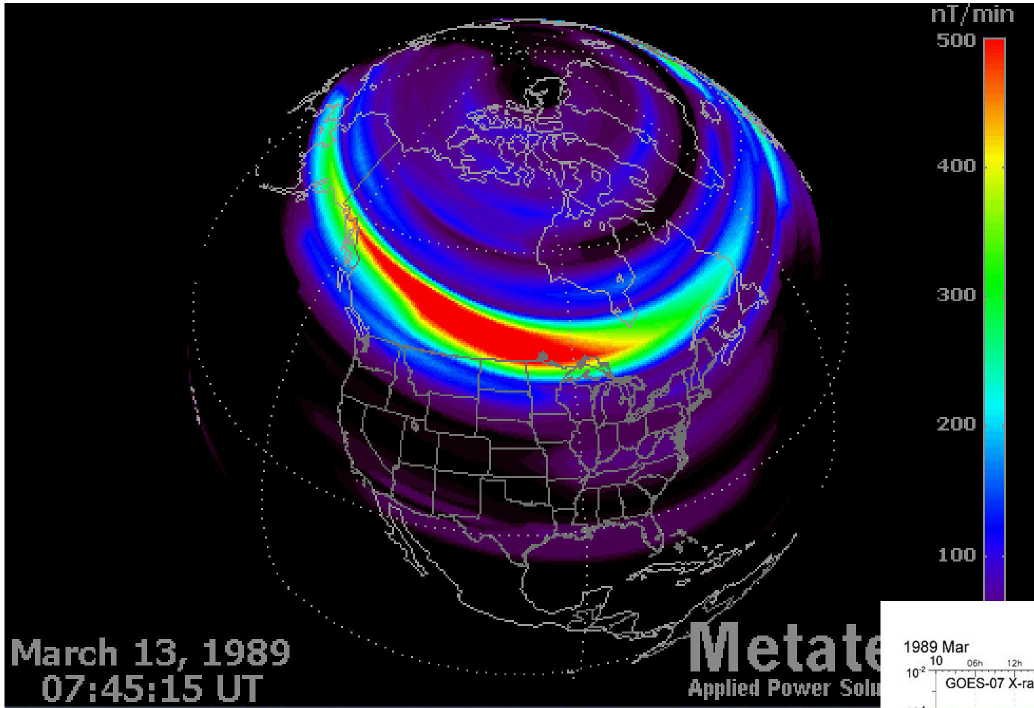
nT/min
500
400
300
200
100
March 13, 1989
07:45:15 UT
Metate
Applied Power Solu

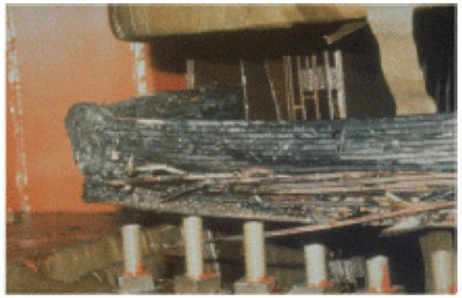


POWER SYSTEM EVENTS DUE TO SMD MARCH 13, 19
B = Blackou
D = Equipme
T = Tripping

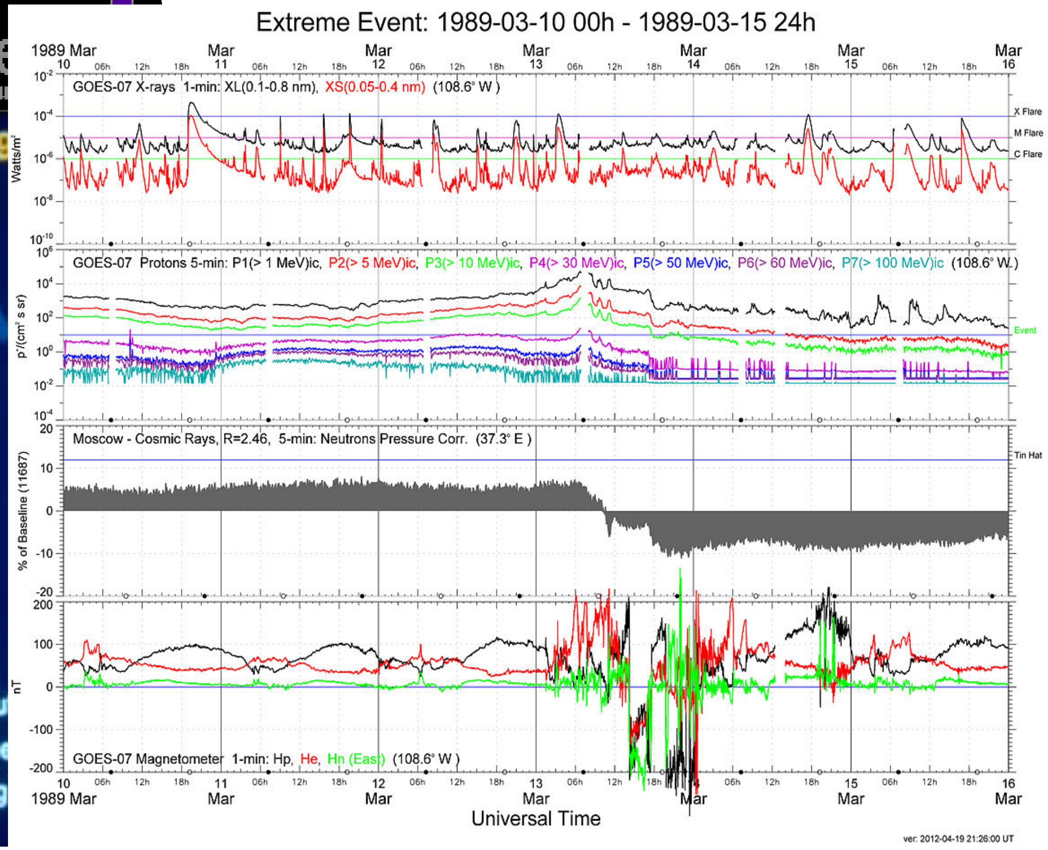
Extreme Event: 1989-03-10 00h - 1989-03-15 24h
GOES-07 X-rays 1-min: XL(0.1-0.8 nm), XS(0.05-0.4 nm) (108.6° W)
X Flare
M Flare
C Flare
Watts/m²
GOES-07 Protons 5-min: P1(> 1 MeV)ic, P2(> 5 MeV)ic, P3(> 10 MeV)ic, P4(> 30 MeV)ic, P5(> 50 MeV)ic, P6(> 60 MeV)ic, P7(> 100 MeV)ic (108.6° W)
Event
Moscow - Cosmic Rays, R=2.46, 5-min: Neutrons Pressure Corr. (37.3° E)
Tin Hat
% of Baseline (11687)
GOES-07 Magnetometer 1-min: Hp, He, Hn (East) (108.6° W)
nT
1989 Mar
Universal Time
ver: 2012-04-19 21:26:00 UT

Space Weather: Global feature

Reported impacts from a storm in October, 2003

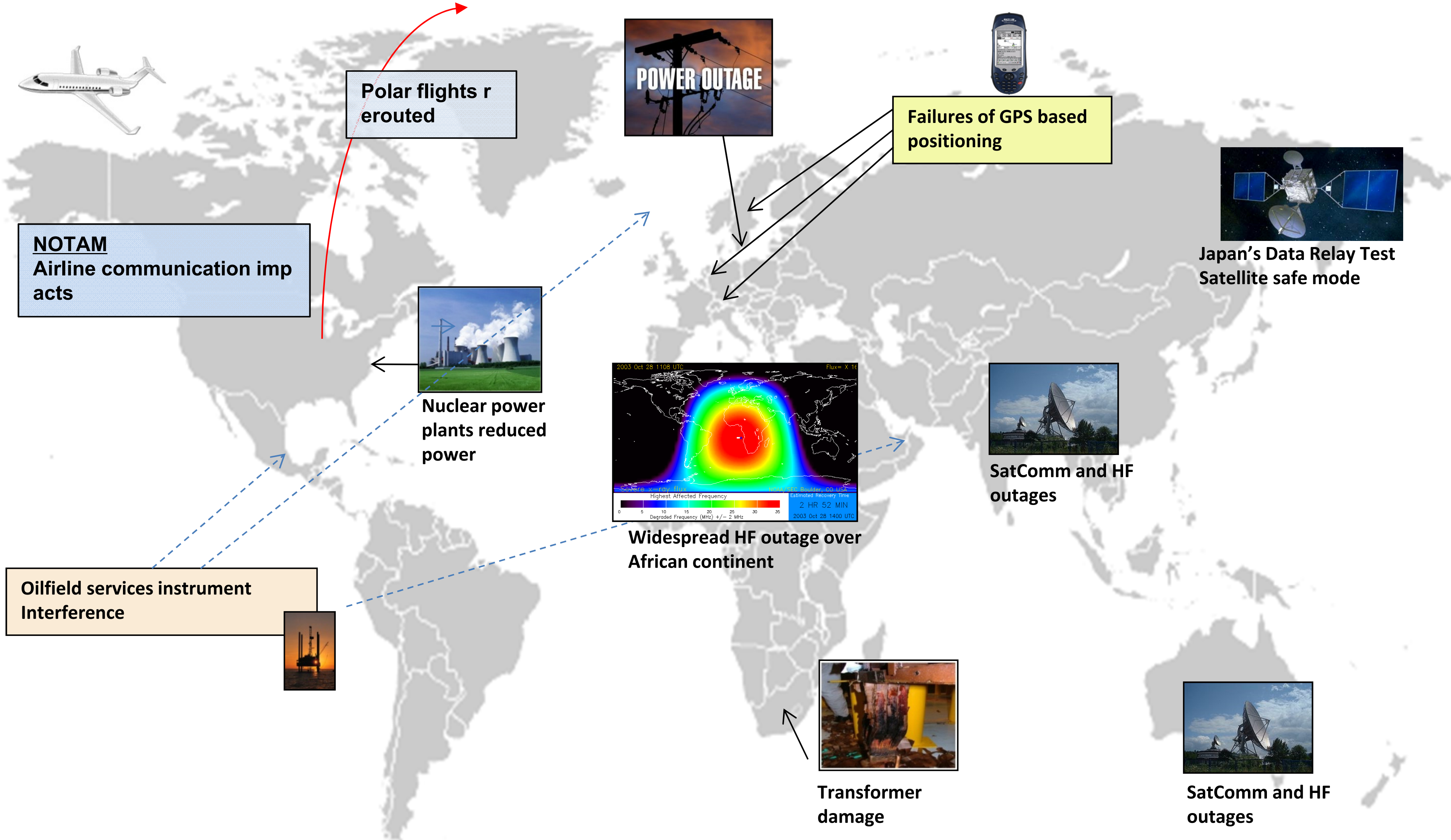

Over 130 hours of HF communication blackout in Anarctic

Home | Help

ISES

International Space Environment Service

ISES | URSIgram Codes | Reports | Regional Warning Centres | Info | Geo-Calendar

Regional Warning Centres

Print this

- Australia (Sydney)
- Belgium (Brussels)
- Brazil (São José dos Campos)
- Canada (Ottawa)
- China (Beijing)
- Czech Republic (Prague)
- India (New Delhi)
- Japan (Tokyo)

http://www.spaceweather.org/

Summary

- The near-Earth space provides a broad range of temporal and spatial phenomena from single-ptl to MHD, which can be confirmed in *in situ* observations.

- MHD disturbances & waves tend to effectively affect geomagnetic variations in the sense that relatively large-scale EM variations occur with considerable amplitude.

- In terms of spatial and temporal scales over CLIC's criterion, it seems that natural sources from "Space" such as dB~nT over dT~1 sec can be well incorporated (Space Weather should be monitored, though).

- In addition, local conductivity variation should be checked in advance by comparing B(t) at the two "Ground" ends.

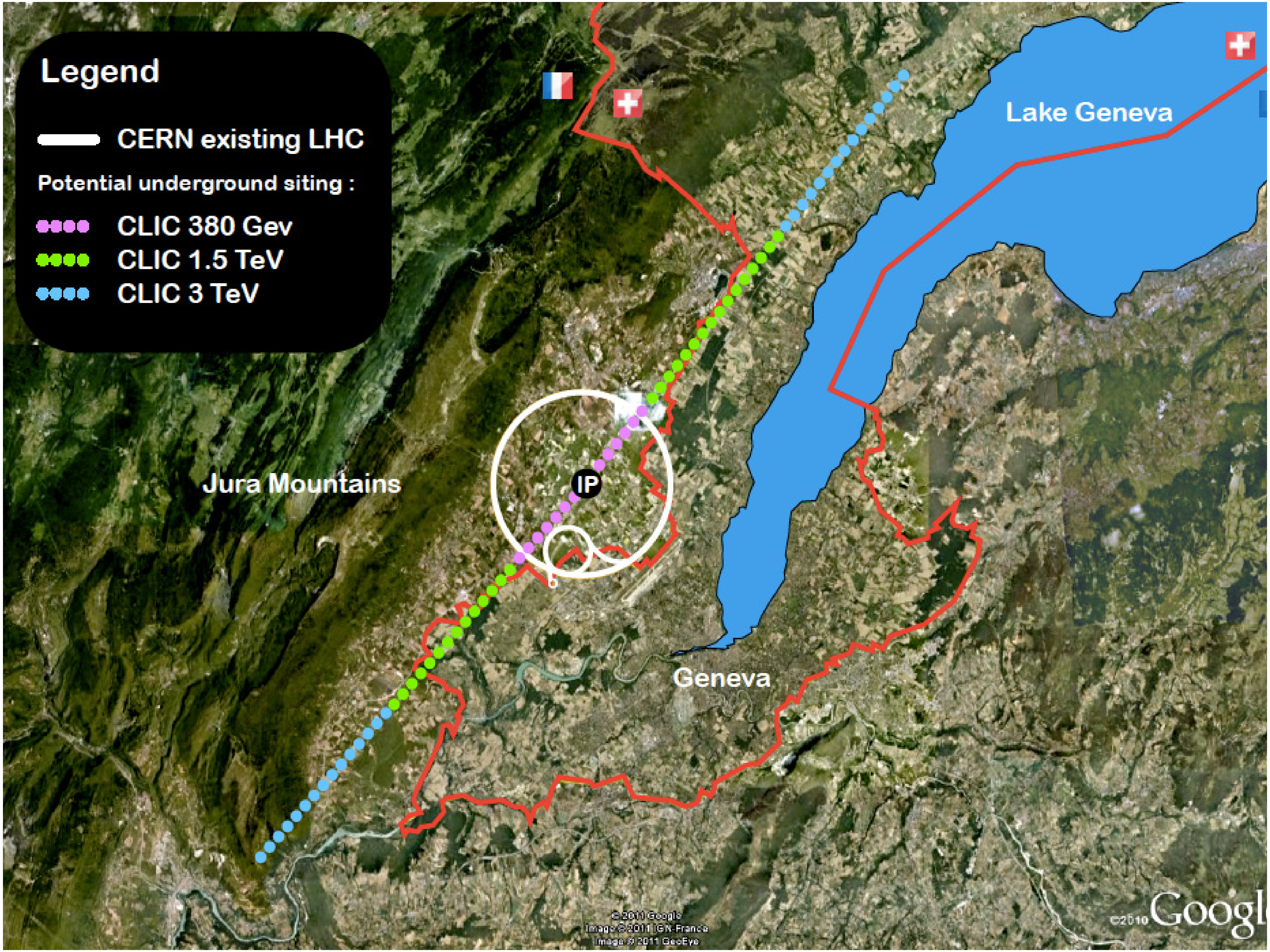
Legend
CERN existing LHC
Potential underground siting :
CLIC 380 Gev
CLIC 1.5 TeV
CLIC 3 TeV
Lake Geneva
Jura Mountains
IP
Geneva
© 2011 Google
Image © 2011 IGN-France
Image © 2011 GeoEye